NASA CR-134254
ERIM 31650-152-T

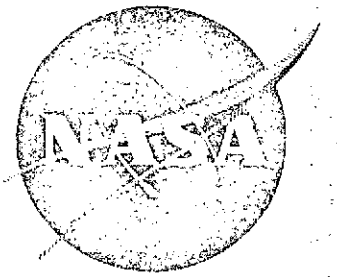

SIGNATURE EXTENSION: AN APPROACH TO OPERATIONAL MULTISPECTRAL SURVEYS

by

R. F. Nalepka and J. P. Morgenstern
Infrared and Optics Division

ENVIRONMENTAL RESEARCH INSTITUTE OF MICHIGAN
FORMERLY WILLOW RUN LABORATORIES, THE UNIVERSITY OF MICHIGAN

prepared for

NATIONAL AERONAUTICS AND SPACE ADMINISTRATION

Johnson Spacecraft Center
Earth Observations Division
NAS9-9784

NOTICES

Sponsorship. The work reported herein was conducted by the Environmental Research Institute of Michigan for the National Aeronautics and Space Administration, Johnson Spacecraft Center, under Contract NAS9-9784, Task B2.11. Dr. Andrew Potter (TF3) of the Earth Observations Division is Technical Monitor. Contracts and grants to the Institute for the support of sponsored research are administered through the Office of Contracts Administration.

Availability Notice. Requests for copies of this report should be referred to:

National Aeronautics and Space Administration
Scientific and Technical Information Facility
P.O. Box 33
College Park, Maryland 20740

Final Disposition. After this document has served its purpose, it may be destroyed. Please do not return it to the Environmental Research Institute of Michigan.

NASA CR-
ERIM 31650-152-T

INFORMAL TECHNICAL REPORT

SIGNATURE EXTENSION: AN APPROACH TO OPERATIONAL MULTISPECTRAL SURVEYS

by

R. F. Nalepka and J. P. Morgenstern
Infrared and Optics Division

ENVIRONMENTAL RESEARCH INSTITUTE OF MICHIGAN
FORMERLY WILLOW RUN LABORATORIES.
THE UNIVERSITY OF MICHIGAN

prepared for

NATIONAL AERONAUTICS AND SPACE ADMINISTRATION

March 1973

NAS9-9784, Task B2.11

Johnson Spacecraft Center
Earth Observations Division
Houston, Texas

FOREWORD

This report describes part of a comprehensive and continuing program of research in multispectral remote sensing of environment from aircraft and satellites. The research is being carried out for the NASA Manned Spacecraft Center, Houston, Texas, by the Environmental Research Institute of Michigan. The basic objective of this program is to develop remote sensing as a practical tool for obtaining extensive information quickly and economically.

During the past few years, the feasibility of using multispectral remote sensing to provide information concerning a wide variety of land conditions has been shown. Applications for such problems as agriculture census-taking, detection of diseased plants, urban and rural land use studies, detection of air and water pollution and measurement of water depths have been developed. The work reported herein was directed towards development of data processing techniques which will permit large area multispectral surveys to be executed in a timely and cost effective manner.

The research covered in this report was performed under NASA Contract NAS9-9784, Task B2.11. The program was directed by R. R. Legault, Director of the Infrared and Optics Division of the Environmental Research Institute of Michigan, and J. D. Erickson, Principal Investigator and Head of the Multispectral Analysis Section of the Environmental Research Institute of Michigan. The Environmental Research Institute of Michigan's number for this report is 31650-152-T.

ACKNOWLEDGMENTS

The authors wish to acknowledge the direction provided by Mr. R. R. Legault and Dr. Jon D. Erickson. The authors would also like to thank Mrs. Lottie Parker and Miss Darlene Dickerson for their secretarial assistance during the execution of this contract.

ABSTRACT

During recent years the feasibility of using airborne multispectral scanner data and automatic processing systems has been demonstrated for the solution of many resource management problems. However, the processing methods used for the feasibility studies have been too slow and required too much a priori knowledge of the data to be either timely or cost effective if used in an operational system.

Two data processing techniques had been suggested as applicable to the large area survey problem. One suggested approach was to use unsupervised classification (clustering) techniques. Investigation of this method showed that since the method did nothing to reduce the signal variability, the use of this method would be very time consuming and possibly inaccurate as well. The conclusion is that unsupervised classification techniques of themselves are not a solution to the large area survey problem.

The other method investigated was the use of signature extension techniques. Generally speaking, such techniques function by normalizing the data to some reference condition. Thus signatures from an isolated area could be used to process large quantities of data. In this manner, ground information requirements and computer training are minimized.

Several signature extension techniques were tested. The best of these allowed signatures to be extended between data sets collected four days and 80 miles apart with an average accuracy of better than 90%.

CONTENTS

FIGURES

TABLES

SIGNATURE EXTENSION: AN APPROACH TO OPERATIONAL MULTISPECTRAL SURVEYS

1 INTRODUCTION AND SUMMARY

1.1. INTRODUCTION

During recent years the feasibility of using airborne multispectral scanner data collection and automatic processing systems has been demonstrated for providing information required by resource managers in many disciplines. The emphasis of current research efforts at ERIM (formerly the Willow Run Laboratories) has shifted from feasibility demonstrations to the development of an operational, large-area survey system employing multispectral remote sensing techniques.

One of the requirements for an operational multispectral scanner survey system is that it provide the required information in a timely and cost effective manner. The processing approach which has been employed by most investigators during the feasibility demonstration stage has required large amounts of ground truth information. This information has been needed to establish the signatures of the object classes of interest in the scene in order to train the computer to recognize those objects. The three processes--gathering ground information, establishing signatures and training the computer--can be costly and time consuming especially if these operations need to be carried out repeatedly over the area being surveyed. Under those circumstances it may become too costly to process large volumes of data using current methods.

The goal of this study was to help bridge the gap between feasibility studies and operational systems. Whereas the feasibility studies were characterized by the need for large amounts of ground truth, large numbers of signatures to represent the subclasses of the object classes of interest, large amounts of computer time, and a necessity to retrain the computer for every 10-20 miles of flight line of data, the operational system, to be cost effective, must be characterized by small amounts of ground truth, a small group of signatures representative of all objects of interest and a minimization of retraining and processing time for the computer.

To meet the stated goal, we began by examining the manner in which multispectral scanner signals vary as the physical parameters of the data acquisition process vary. With this knowledge as a foundation, we then developed and tested various methods of data processing to determine if they were feasible for use in operational multispectral survey systems.

The methods studied to minimize the computer training and ground data collection effort required for an operational system fell into two broad categories. One approach was to use unsupervised classification techniques (clustering). The other approach was to devise processing techniques which required only one set of signatures gathered from an isolated area to process many data sets. Thus, as the end result of this study, our goal was to identify data processing methods which would allow processing of large amounts of data within an acceptably small time/cost frame.

1.2. SUMMARY

Investigation into the sources of signal variability was carried out. It has shown that atmospheric attenuation and scattering are prominent causes of signal variation. Additional sources of variation include changes in solar conditions, bidirectional reflectance, and scanner electronics.

Two data processing techniques had been suggested as applicable to the large area survey problem. One suggested approach was to use unsupervised classification (clustering) techniques. Investigation of this method showed that, since the method did nothing to reduce the signal variability, the use of this method would require large amounts of processing time in order to obtain reasonable classification accuracy. The conclusion is that clustering techniques of themselves are not a solution to the large area survey problem.

The other method investigated was the use of signature extension techniques. Generally speaking, such techniques function by normalizing the data to some reference condition thus reducing the variability of the data. Thus signatures from an isolated area could be used to process large quantities of data. In this manner ground information requirements and computer training are minimized.

Several signature extension techniques were devised and tested. The first of these was the ratio of adjacent channels transformation which yielded fair to good results. However, it was decided that classification

accuracy for this transformation could be increased if the path radiance effects could first be eliminated from the data.

Accordingly, attempts were made to estimate the path radiance effects in the data. One method used the ERIM radiative transfer model to calculate the path radiance. Because of problems associated with the calibration of the data or with the specification of parameters to the model, this approach was unsuccessful. A second, empirical approach was devised. In this approach, the smallest signals at each scan angle were used as an estimate of path radiance. Results of classifying data modified in this manner were inconclusive. These two approaches should have, theoretically, improved classification accuracy. We feel that these initial test results may not be indicative of the ultimate utility of these approaches.

Other signature extension techniques tested were the U-V transformation and the average signal versus angle transformation. The U-V transform yielded good results in a limited test. Results of the average signal versus angle transform were excellent.

The best signature extension technique tested was the average signal versus angle approach. This technique allowed signatures to be extended over a 90^{o} scanner field of view and between data sets collected four days and 80 miles apart with an average accuracy of better than 90%.

MULTISPECTRAL SCANNER DATA VARIABILITY

In this section we present a brief discussion of the factors which affect the radiation sensed by a multispectral scanner. The problems associated with the automatic processing of large area surveys will become more apparent when the variability of scanner data is better understood.

Simply speaking, the radiation being sensed by the multispectral scanner in each spectral band is given by

$$L_o = \rho E T + L_p \tag{2.1}$$

where the target, exhibiting a reflectance ρ for the existing scanner-target-sun geometry, has an irradiance E incident upon it. The radiance reflected in the direction of the scanner (ρE) is then attenuated by a factor T as it traverses the atmospheric path between the ground and the scanner. There is also a contribution by radiation which is scattered into the scanner field of view. This quantity, the path radiance (L_p) is added to the radiation reflected from the target. Thus, the radiance observed at the scanner (L_o) consists of radiation reflected by the target as modified by both additive and multiplicative factors.

Multispectral remote sensing is based on the premise that associated with most object classes is a unique vector of reflectances (ρ). The first problem in recognition processing arises because the scanner senses not ρ, but L_o. Moreover, and this is a second problem, the values of E, T, and L_p are not constant over the whole data set. They will vary. Let us next examine why these three quantities vary and to what extent.

There are a large number of factors which can be sources of variation in scanner signals. Some of these sources are listed below, where we have broken them down into three categories: instrumental sources, environmental sources, and scene related sources of variation.

SOURCES OF VARIATION IN MULTISPECTRAL SCANNER SIGNALS

A. Instrument
   - Scanner Electronics and recorder instabilities
   - Gain changes
   - Nonuniform angular responsivity

B. Environment
   - Changes in irradiance
   - Changes in atmospheric transmittance
   - Changes in atmospheric path radiance

C. Scene
   - Geometric effects
   - Reflectance effects

Instrumental sources are associated with the mechanics, optics, and electronics of the multispectral scanner. Included in this category are gain changes, non-uniform angular responsivity, and other recorder and electronic instabilities. Since many of these effects are deterministic, they can be eliminated from the data during an initial data preparation stage.

Environmental sources of variation include changes in the magnitude and spectral make-up of the irradiance at ground-level, changes in atmospheric transmittance, and changes in path radiance. Changes in irradiance result from changes in the atmospheric state (i.e., the type, number, and location of clouds and the existance of other absorbing and scattering aerosols and gasses) as well as from solar positional changes that occur during or between the times area survey data sets are collected.

Atmospheric transmittance and path radiance will also change as the atmospheric state changes. These quantities are also functions of scan angle since they vary depending on the path length from the ground to the scanner. An example of the effect of angular variation on atmospheric transmittance is shown in Figure 1. It can be seen that the effect is largely parabolic and symmetric around the nadir. The information shown here was computed using a radiative transfer model developed at ERIM.[1]

Model calculations are seen in Figure 2 for variation in path radiance as a function of scan angle and time of day for an East-West flight direction. Path radiance increases rapidly near the extreme scan angles. When the angle of view of the scanner is opposite the sun, the path radiance reaches a local maximum. This is seen in Figure 2 as occuring near noon.

The quantities T and L_p will vary with scan angle over a single scan line and the quantities E, T, and L_p may vary during the time a data set is collected. Therefore, the signal generated when viewing a single object class may exhibit a wide range of multivariate values. Under such conditions, different object classes viewed at various locations in the data set may result in identical scanner signals. Thus, for example, the same scanner signal may be generated for object class 1 at one location, object class 2 at a second location, object class 3 at a third...etc. Obviously, under such conditions obtaining accurate recognition results may not be possible. The situation becomes even more acute when one considers the variations in E, T and L_p that may occur between data sets.

Even if the variations associated with the atmosphere were eliminated, there still would be other potential sources of variation or change in the radiance observed when viewing any one object class on the ground. First

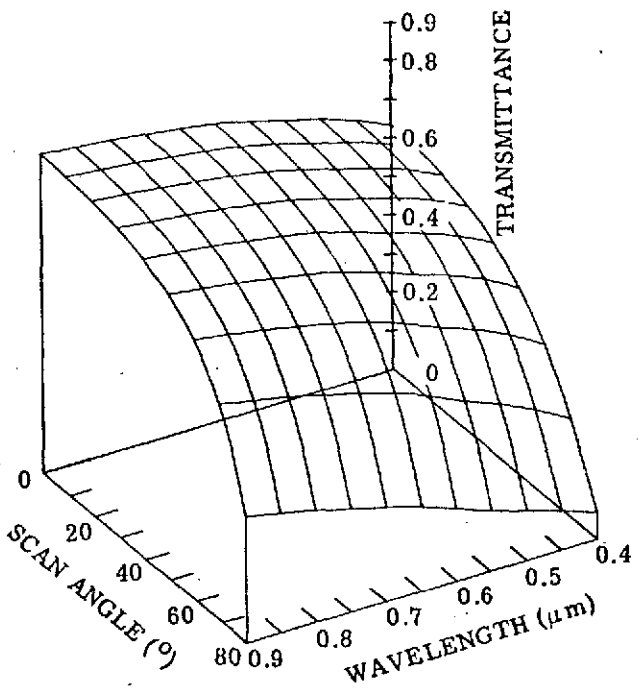

FIGURE 1. DEPENDENCE OF TRANSMITTANCE ON WAVELENGTH AND SCAN ANGLE. Visual range = 8 km; altitude = 1 km.

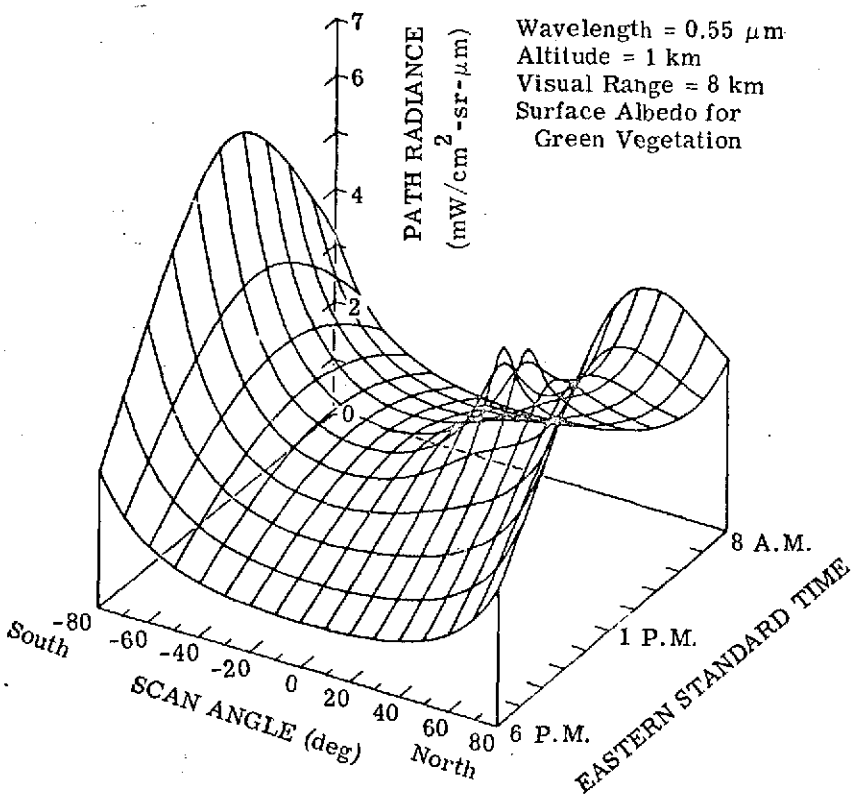

FIGURE 2. DEPENDENCE OF PATH RADIANCE ON TIME AND SCAN ANGLE. Southeastern Michigan, 1 September 1971.

of all, most objects of interest are geometrically complex (e.g., corn plants). Because of this complexity the elements of such objects being illuminated by direct sunlight (the primary source of radiation) depends on the location of the sun in the sky. Some elements may be illuminated at certain times of the day or year and not at others. Similarly, depending on the location of such objects under the scanner aircraft, certain elements may or may not be visible to the scanner. Clearly such effects will cause variations in the radiance observed.

Another scene-related source of variation is associated with the reflectance characteristics of the object being viewed. Since most object materials are not Lambertian reflectors, there will be a nonuniform distribution of radiation reflected from them. This will occur independent of the geometric effects. Therefore, the radiance observed when viewing a geometrically simple object or material (e.g., a field of bare soil, a paved road, or a calm body of water) will be a function of the view angle as well as the angular distribution of radiation incident upon that object. Of course, this is also true for geometrically complex objects.

Except for the deterministic instrumental variations, the other variations are interrelated to a great extent. For instance, a change in atmospheric state will cause changes at any particular wavelength in both the magnitude and the spatial distribution of the incident irradiance. Because of the change in the spatial distribution of incident radiation, the radiation reflected in the direction of the sensor will be modified additionally due to purely geometric effects as well as the non-Lambertian character of the object

being viewed. This reflected radiation will then be attenuated to a lesser or greater extent before reaching the sensor while at the same time more or less path radiance will be incident at the sensor altitude. So, theoretically, a relatively small change in atmospheric state could result in a potentially significant change in the radiation detected by the sensor.

To evaluate the extent of the effects of these variations in real data, we selected for study three of the Corn Blight Watch Experiment data sets gathered during Mission 43M. These data sets were collected over three test areas in western Indiana and bear the designations Segments 204, 203, and 212. The data were digitized, and prepared to eliminate or reduce variations due to instrumental effects, and were then calibrated in terms of radiance. (See Appendix I for a description of the data processing program.)

Areas containing corn, soybeans, and trees (the major ground covers) were located in the data for each of the segments. In order to determine the magnitude of the scan angle variations, the mean radiance values associated with samples of each of these ground covers were calculated as a function of scan angle for each data set. The results for two scanner wavebands of Segment 204 are shown in Figures 3 and 4. It is apparent on examining these figures that there is no means of clearly delineating any of the object classes for all (or most) scan angles using a single signature for each object class. These two bands are typical for all the wavebands for each of the three data sets studied. These results are completely in line with previous

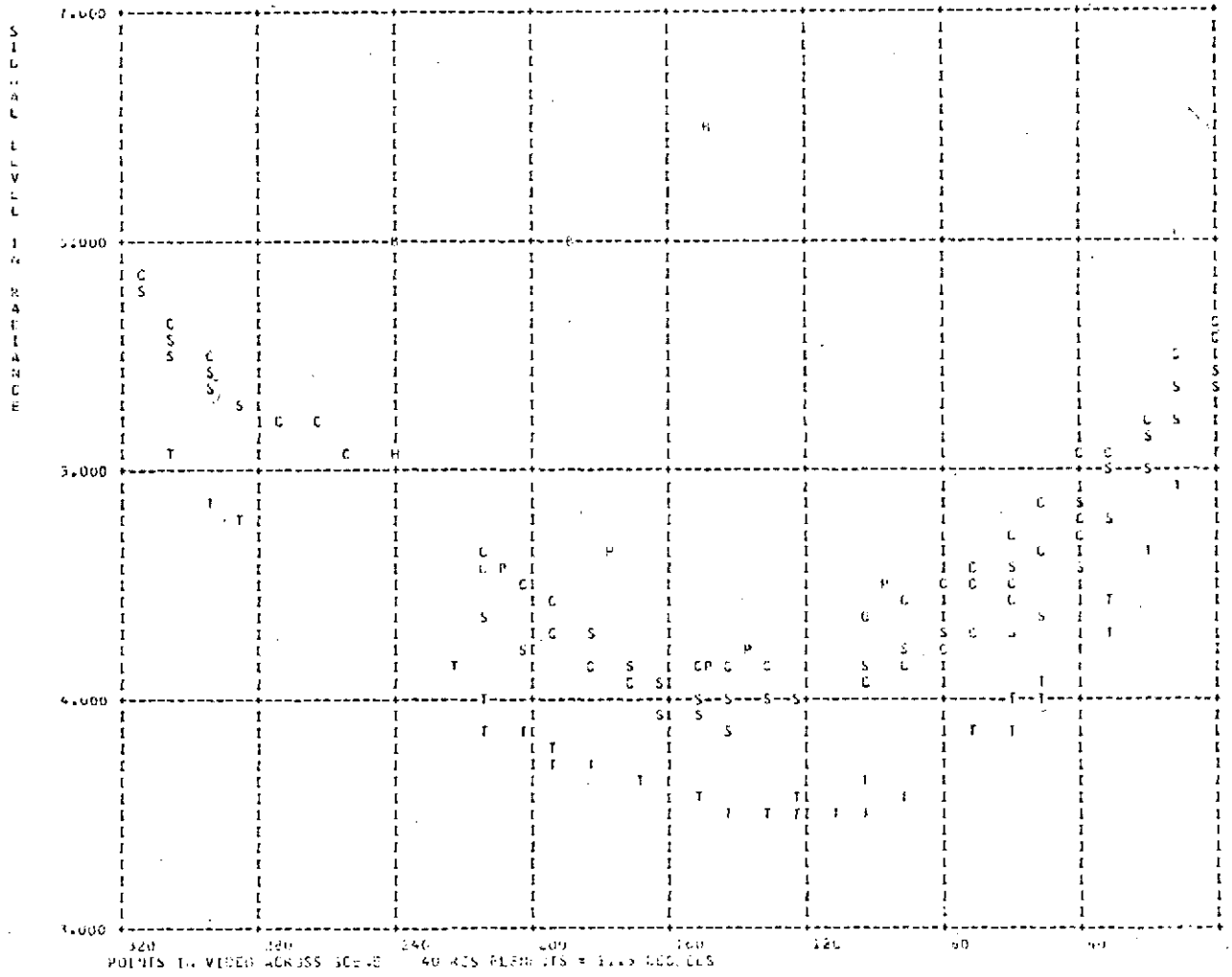

FIGURE 3. VARIATION OF SPECTRAL RADIANCE AS A FUNCTION OF SCAN ANGLE FOR CORN, SOYBEANS, AND TREES FOR SEGMENT 204, MISSION 43M. Untransformed data. Channel = 0.46-0.49 μm.

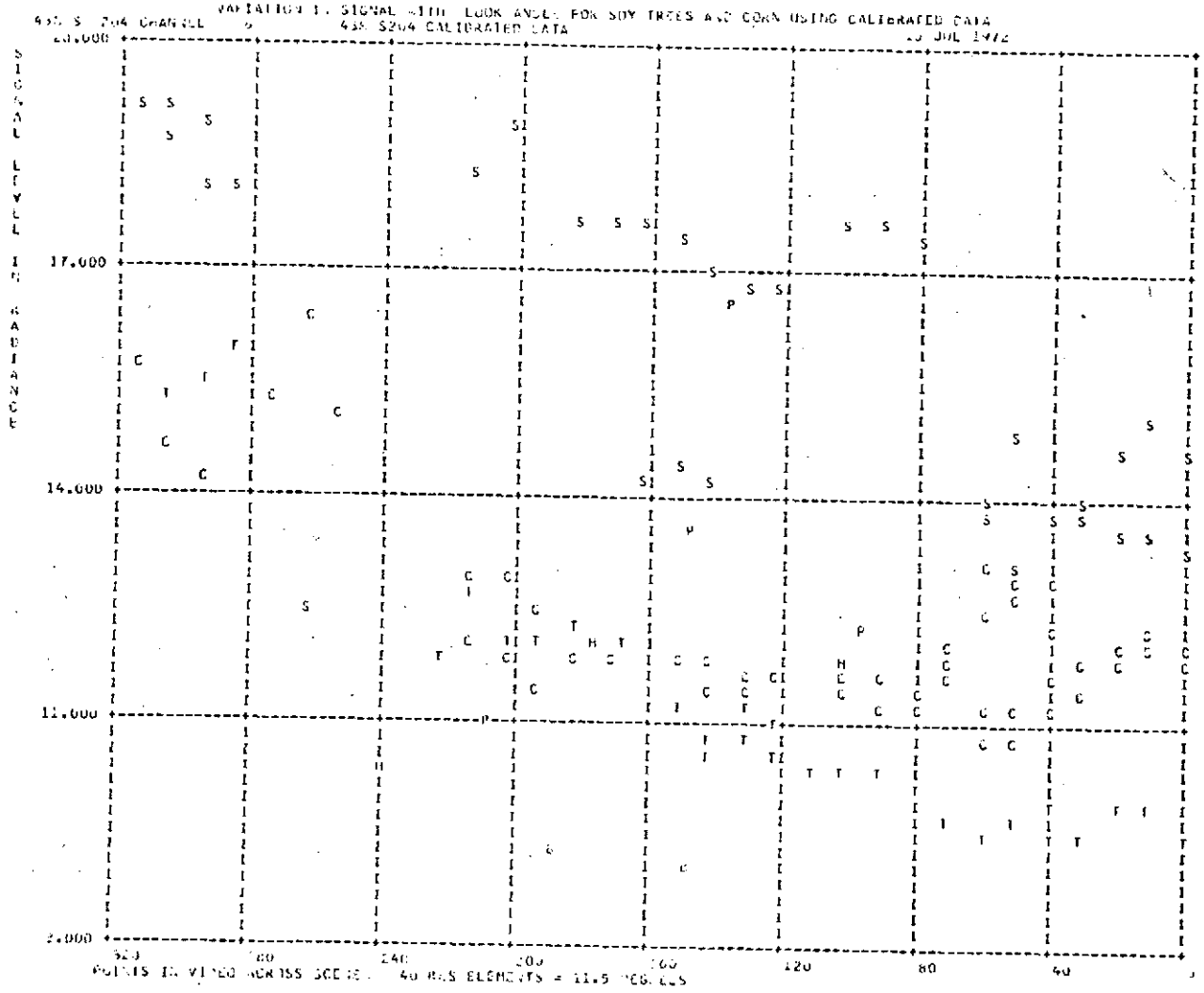

FIGURE 4. VARIATION OF SPECTRAL RADIANCE AS A FUNCTION OF SCAN ANGLE FOR CORN, SOYBEANS, AND TREES FOR SEGMENT 204, MISSION 43M. Untransformed data. Channel = 0.72-0.92 μm.

experience: Raw multispectral scanner data has embodied in it a great deal of angular variation. That this variation is sufficient to cause confusion and poor results in the classification process is shown in the following sections.

3
UNSUPERVISED CLASSIFICATION APPROACH

The use of unsupervised classification techniques (i.e., clustering) has been mentioned in several quarters as the solution to the problems posed by an operational remote sensing system.[2]

In the clustering approach, the set of multispectral scanner data points to be processed are examined and distinct groupings or clusters of data points are identified. Each of these clusters are then used to establish training signatures for the computer. Only after the data set has been classified into the many clusters is the ground information gathered to associate a real object with each of the clusters.[2,3,4,5] As the theory goes, only a minimal amount of ground information need be gathered since the clusters classification results can be used to direct the ground truth team to only a few locations in the survey area to determine the correspondence between clusters and real objects. We feel that this approach is a very reasonable one, except that it seems to overlook the very real problem of signal variation.

As an example, we chose data points from one data set (Segment 204) representing the three object classes at five different scan angles: 0^{o}, $\pm 25^{o}$, $\pm 40^{o}$ from nadir. Attempts to generate three clusters (after all, there are only three classes represented) resulted, as Table I below shows, in the points being clustered according to their location in the scene, rather than according to object class.

TABLE 1. RESULTS OF CLUSTER ANALYSIS USING THREE CENTROIDS FOR CORN, SOYBEANS AND TREES AT 0°, $\pm 25^{\circ}$, $\pm 40^{\circ}$

(Numbers are % of category in cluster)

Class	Scan Angle	Cluster # 1	2	3
Corn	-40°	100		
Soybeans	-40°	100		
Trees	-40°	40	60	
Corn	-25°	100		
Soybeans	-25°		100	
Trees	-25°		100	
Corn	0°	95	5	
Soybeans	0°		100	
Trees	0°		100	
Corn	25°			100
Trees	25°			100
Corn	40°			100
Soybeans	40°			100
Trees	40°			100

Obviously, the variation in signals caused by the environmental and/or scene-related effects overshadowed any differences in the basic reflectance spectra of these ground covers. Further experiments revealed that it took eight clusters to correctly separate the three object classes as shown in Table 2; the resultant error rate (points assigned to the wrong cluster) was about 3%.

TABLE 2. RESULTS OF CLUSTER ANALYSIS USING EIGHT CENTROIDS FOR CORN, SOYBEANS AND TREES FOR SEGMENT 204 AT SCAN ANGLES 0°, $\pm 25^{\circ}$, $\pm 40^{\circ}$

(Numbers are % of category in cluster)

Class	Scan Angle	Cluster #							
		1	2	3	4	5	6	7	8
Corn	-40°	-	100	-	-	-	-	-	-
Corn	-25°	-	100	-	-	-	-	-	-
Corn	0°	-	100	-	-	-	-	-	-
Corn	25°	100	-	-	-	-	-	-	-
Corn	40°	100	-	-	-	-	-	-	-
Soybeans	-40°	-	-	-	100	-	-	-	-
Soybeans	-25°	-	-	-	-	100	-	-	-
Soybeans	0°	-	-	-	-	100	-	-	-
Soybeans	40°	-	-	100	-	-	-	-	-
Trees	-40°	-	42	-	-	-	58	-	-
Trees	-25°	-	-	-	-	-	100	-	-
Trees	0°	-	-	-	-	8	92	-	-
Trees	25°	-	-	-	-	-	-	52	48
Trees	40°	-	-	-	-	-	-	57	43

Error Rate = 3.6%

Now the question is asked, is it cost effective to use eight signatures (as represented by the clusters) to classify three object classes? This is roughly a threefold increase in time to train the computer and at least a threefold increase in processing time and ground truth necessary to accurately classify the data. The answer to the question appears to be that such an approach is not cost effective.

Nor is the clustering approach to be faulted only on this score. This approach proves to be cumbersome on many other counts as well. Because of its nature, the clustering process must be carried out for each of the data sets to be processed. Also, the clustering process itself is fairly time consuming because the algorithms used tend to be complicated, frequently involving several passes through all the data to be classified with tentative merging and partitioning of the data sets. In addition, most of the current clustering algorithms require additional information, such as the expected number of clusters or the size and shape of the clusters, that may not be available in an operational environment. One last, perhaps minor, fault is that the ground truth is gathered only after classification. In some instances the characteristics of certain areas may be different at ground information collection time than they were at data collection time. For example, in an agricultural scene, fields may be cut, harvested, plowed, or (early in the growing season) exhibit a marked increase in ground cover -- all these changes occurring during the time the data set is being processed.

Thus, the unsupervised classification approach by itself does not appear to meet the requirements for an operational processing system. It requires retraining for every data set; the process of extracting the signatures (clusters) is a time consuming process requiring additional information that may not be available. Because of variation in the scanner generated signals it requires many more times the number of signatures than there are object classes, with a resulting manyfold increase in actual processing time. Finally, the accuracy of the ground truth may be in doubt.

4
SIGNATURE EXTENSION

It is evident from the above discussion that many sources of variation are manifest in the data. Moreover, the variation in scanner signals is large enough to obscure the spectral differences of the object classes being scanned. Because of these variations, the clusters or spectral signatures associated with each object class are often limited in their applicability over time and space -- even over a single scan line in many instances. Thus, we believe that for efficient large scale processing of multispectral data, the systematic environmental effects in the data cannot be ignored. We have therefore concentrated our effort on devising and testing data processing techniques that will reduce or eliminate these effects in the data.

At ERIM a great deal of research has been carried out over the last few years to develop techniques that eliminate (or reduce) the variations in scanner signals which degrade classification accuracy.[6,7,8] These techniques have become known as preprocessing transformations (because in many of them the data is transformed before classification processing) or signature extension techniques. However, since we want to extend the applicability of a signature over all scan angles, over all scan lines in a data set, and over several data sets, we feel that the term signature extension is more appropriate.

To demonstrate the kind of results that may be achieved by applying signature extension techniques we repeated the experiments described earlier in this report.

In contrast to Figures 3 & 4 which were discussed in Section 2, Figures 5 and 6 show the same two wavebands after the data were transformed

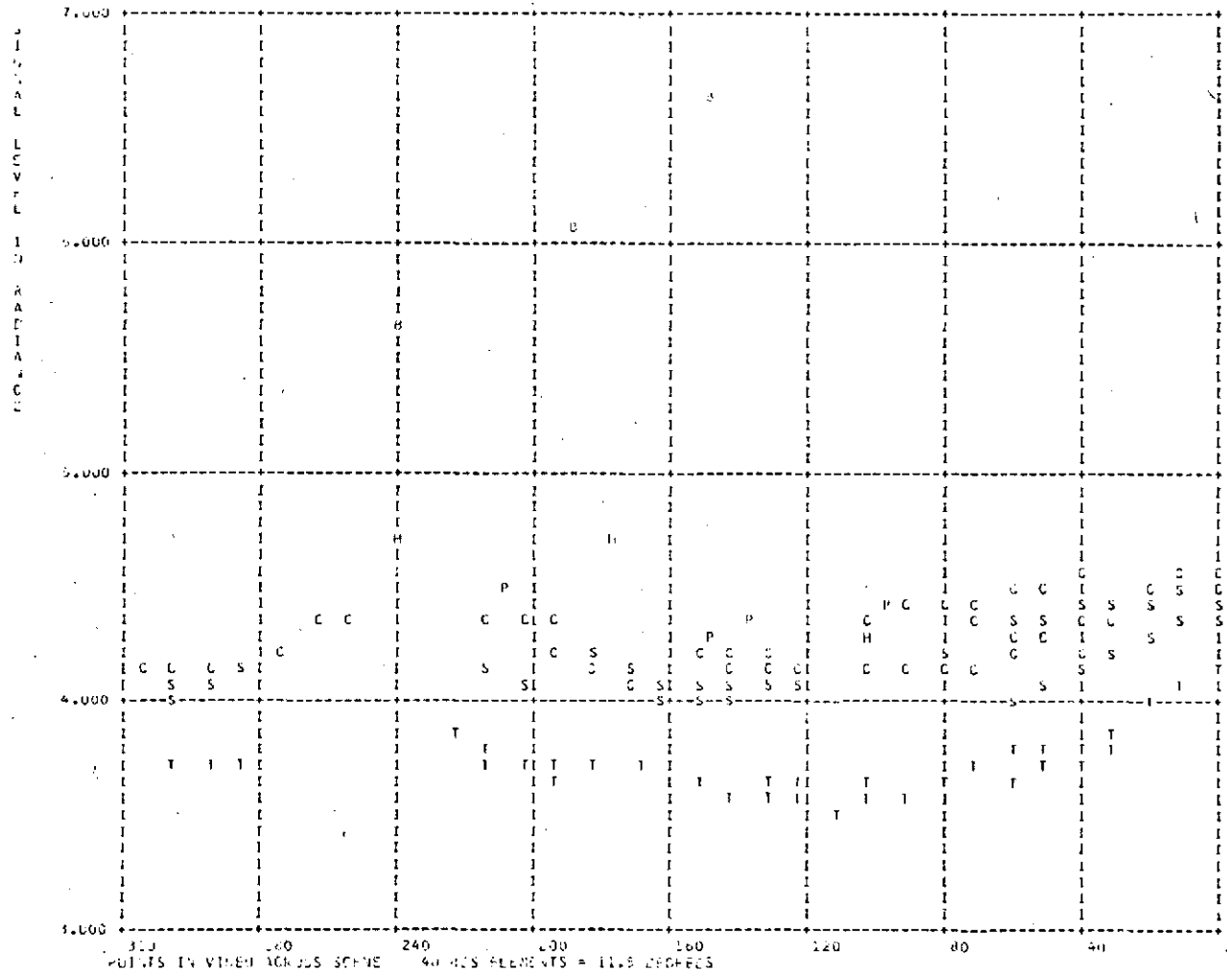

FIGURE 5. VARIATION OF SPECTRAL RADIANCE AS A FUNCTION OF SCAN ANGLE FOR CORN, SOYBEANS, AND TREES FOR SEGMENT 204, MISSION 43M.
Data transformed using average signal vs. angle transform.
Channel = 0.46-0.49 μm.

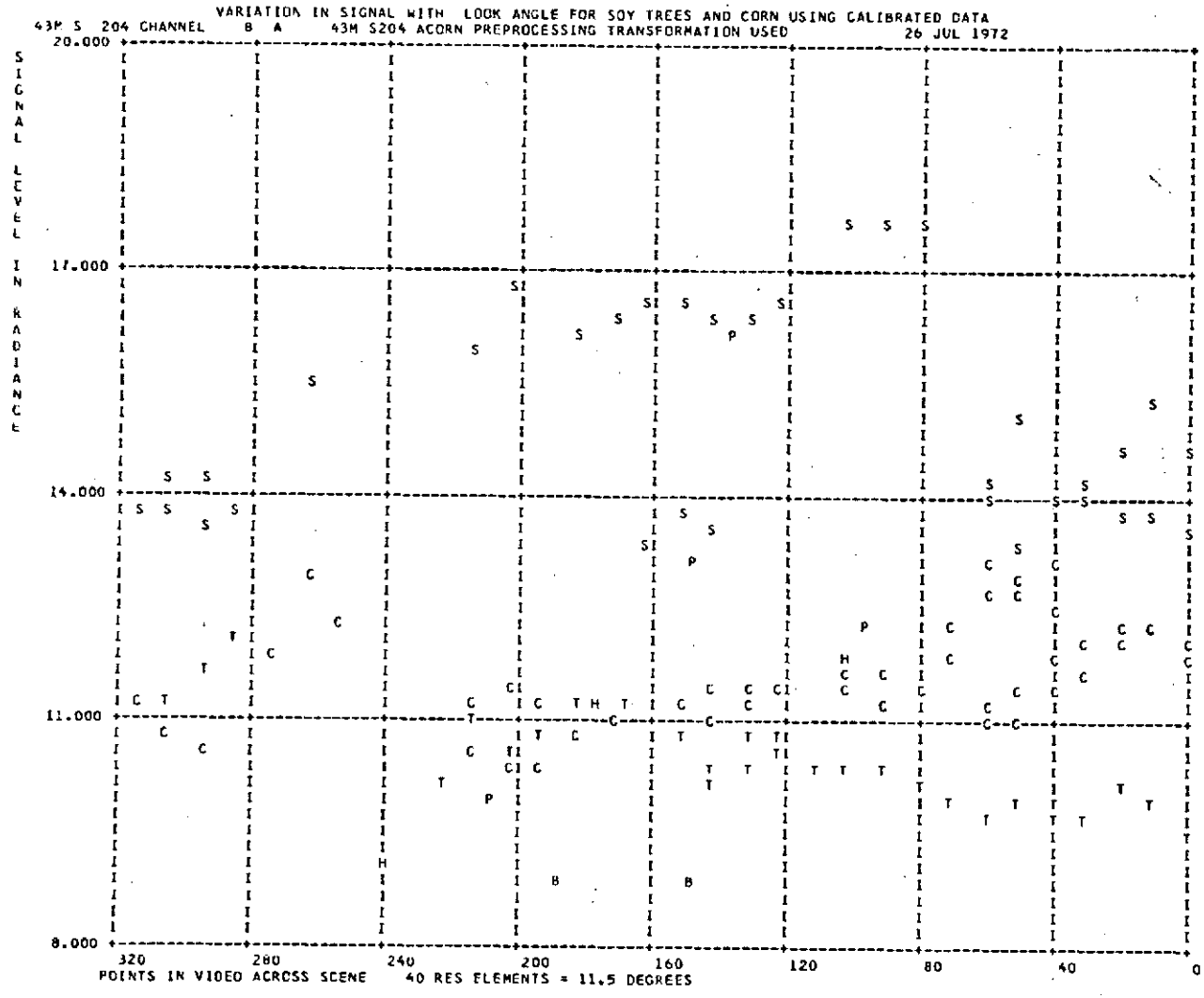

FIGURE 6. VARIATION OF SPECTRAL RADIANCE AS A FUNCTION OF SCAN ANGLE FOR CORN, SOYBEANS, AND TREES FOR SEGMENT 204, MISSION 43M.
Data transformed using average signal vs. angle transform.
Channel = 0.72-0.92 μm.

using one of the available signature extension transforms (in this instance the average signal vs angle transform). Here, there is practically no hint of angular variation. It is apparent that separability between object classes is such that only one training set for each object class would be necessary for satisfactory recognition processing over all scan angles. A repeat of the clustering experiment reported in Section 3 using transformed data showed that the data successfully clustered into only three groups with a 7% error rate. The results of this experiment are shown in Table 3.

TABLE 3. RESULTS OF CLUSTER ANALYSIS USING TRANSFORMED DATA AND THREE CENTROIDS FOR CORN, SOYBEANS, AND TREES FOR SEGMENT 204 AT SCAN ANGLES 0°, $\pm 25^{\circ}$, $\pm 40^{\circ}$

(Numbers are % of category in cluster)

Class	Scan Angle	Cluster # 1	2	3
Corn	-40°	100	-	-
Corn	-25°	100	-	-
Corn	0°	100	-	-
Corn	25°	100	-	-
Corn	40°	99	-	1
Soybeans	-40°	-	100	-
Soybeans	-25°	-	100	-
Soybeans	0°	-	82	18
Soybeans	25°	-	100	-
Soybeans	40°	-	100	-
Trees	-40°	17	19	64
Trees	-25°	-	2	98
Trees	0°	-	5	95
Trees	25°	-	34	66
Trees	40°	-	8	92

Error Rate = 7%

While this is only one example of the improvement obtained by application of signature extension techniques, it is nevertheless indicative of the kinds of results observed for the more successful signature extension techniques tested.

In the remainder of this report, we will describe and report on the various signature extension techniques that were tested. In all cases, the tests were carried out as follows: First, the particular transformation being studied was applied to the three data sets being used for this investigation. A one square mile area of Segment 204, which was within $\pm 30°$ of nadir, was used for training. Seven major object classes were identified in this area (corn, soybeans, pasture, cut hay, hay, trees, and sparse vegetation) and signatures were extracted for each of them. These signatures were then used to process all of Segment 204, and Segments 203 and 212. A more detailed discussion of the training procedure can be found in Appendix I.

A summary of the conditions existing at the time of data collection for the three data sets is presented in Table 4.

TABLE 4

SUMMARY OF MEASUREMENT CONDITIONS
FOR SEGMENTS 203, 204, 212, MISSION 43M

	Segment 203	Segment 204	Segment 212
Latitude	41°36'	41°12'	40°3'
Longitude	86°32'	87°28'	86°49'
Date of Flight	8/13/71	8/13/71	8/17/71
Time of Flight	1053 EST	1025 EST	1120 EST
Solar Azimuth	127°	118°	137°
Solar Elevation	53°	48°	57°
Visibility	14.5 KM		21 KM
Cloud Cover	Clear	Clear	Clear

We want to emphasize the point that the processing approach was not specially designed to produce good results. The training area was selected principally because a number of fields of each object class was present. Only one classification pass was made for each data set; in no instance were any parameters or signatures changed and then classification carried out for a second time. It is quite conceivable that better results could have been obtained by taking advantage of the information we had on the remainder of the data to be processed. However, the processing was carried out in a manner simulating the circumstances of a large scale survey where such attention to individual data sets would not be possible.

To evaluate and compare results from the various transforms tested, a large number of test fields were defined for each segment. To further monitor any latent angular variation in the data, the test fields were divided into "middle" and "edge" categories, depending on their position in the scene. For Segment 204, edge fields were those that were located at scan angles from 30° to 45° from nadir. For Segments 212 and 203, such fields were located at scan angles between 20° - 30° from nadir. (The difference in the definition of edge fields reflects a difference in the amount of the scanner field of view which was digitized for the three data sets.) All results reported herein refer to the classification accuracies of the data points in these fields.

For the first test, no transformation was applied to any of the data sets. The signatures obtained from Segment 204 were used to classify all three data sets. The results of this classification are shown in Table 5. Here we see that the classification accuracy for the middle area of Segment 204 was quite high. However, the recognition results for data outside the central 60° of the

scanner field were very poor. Thus, without preprocessing, accurate recognition was obtained for less than two-thirds of each scan line for the same data set from which the signatures were extracted. The results of applying the same signatures during the classification of the other two segments were very poor. For neither Segments 203 or 212 is the classification accuracy high enough to be acceptable. It seems that most of Segment 203 was classified as being trees. It is especially noteworthy that the results for Segment 203 are so poor, as this data set was collected only 30 minutes after Segment 204 data.

TABLE 5. CLASSIFICATION RESULTS FOR UNTRANSFORMED CASE. ALL DATA CLASSIFIED USING SIGNATURES FROM SEGMENT 204.

	% Recognition for Test Fields		% False Alarm Rate for Test Fields
	Middle	Edge	
Segment 204			
Corn	93	70	0.9
Soybeans	84	12	8.7
Trees	90	20	1.4
Segment 203			
Corn	9	1	0
Soybeans	5	4	0
Trees	62	61	88.0
Segment 212			
Corn	35	38	1.2
Soybeans	36	36	17.0
Trees	67	84	9.3

The purpose of this test case was to show that the data must be corrected for environmental effects in order for signatures to be successfully extended over a wider scanner field of view or to several data sets.

The following subsections describe several signature extension methods tested and an evaluation of the results using these methods.

4.1. RATIO TRANSFORMATIONS

Ratio transformations are a class of data transformations that utilize ratios between components of each data point so as to normalize that data point. Since the properties of the environment which cause data variability are reflected in the data, it may be possible to reduce the effect of the variability by ratioing data components. A number of possible ratios may be considered. In this report we limit outselves to the discussion of only two of those possibilities.

4.1.1. RATIO OF ADJACENT CHANNELS.

The ratio transformation discussed in this section is the ratio of adjacent channels.[6,7] The basis for the ratio of adjacent channel transform is the effect that, for any given set of conditions, the variations in the multiplicative effects in adjacent spectral regions tend to be highly correlated. That is, for the i^{th} and $(i+1)^{th}$ channels the ratio:

$$\frac{E_{i+1}T_{i+1}g_{i+1,j}}{E_iT_ig_{i,j}} \approx \text{CONSTANT} \qquad (4.1)$$

where E is the irradiance, T is the transmission and g is the angular reflectance function for the particular ground cover j.

The ratio of adjacent channels i and (i+1) yields:

$$R_i = \frac{L_{o_{i+1}}}{L_{o_i}} = \frac{\rho_{i+1,j} E_{i+1} T_{i+1} g_{i+1,j} + L_{p_{i+1}}}{\rho_{i,j} E_i T_i g_{i,j} + L_{p_i}} \tag{4.2}$$

and if the path radiance term can be ignored

$$R_i = \frac{\rho_{i+1,j} E_{i+1} T_{i+1} g_{i+1,j}}{\rho_{i,j} E_i T_i g_{i,j}} \tag{4.3}$$

or

$$R_i \approx \frac{\rho_{i+1,j}}{\rho_{i,j}} * (\text{CONSTANT}) \tag{4.4}$$

Thus the resulting transformed data point is a function only of the reflectance properties of the area being imaged and is not scan angle dependent.

Computationally, this transformation has several advantages in that it requires no a priori knowledge of the specific form of variations in the data nor are there any necessary parameters to be calculated for it. Also, it allows signatures to be simply extended to other data sets. Since all changes in illumination and transmittance between (or within) data sets should be accounted for in the ratio, the ratio signatures from Segment 204 were used to process the other two segments without any modification whatsoever.

Results obtained utilizing this approach were good. Percentage correct classification for Segment 204 was roughly 80%, for Segment 212 about 75%, and for Segment 203 about 65%. Reference is made to Table 6 for exact results of recognition accuracy and false alarm rate.

TABLE 6. CLASSIFICATION RESULTS FOR RATIO OF ADJACENT CHANNEL TRANSFORMATION. ALL DATA CLASSIFIED USING SIGNATURES FROM SEGMENT 204.

	% Recognition for Test Fields		% False Alarm Rate for Test Fields
	Middle	Edge	
Segment 204			
Corn	95	98	3.0
Soybeans	90	57	2.5
Trees	93	55	4.0
Segment 203			
Corn	90	94	5.0
Soybeans	8	28	0.6
Trees	68	75	76.0
Segment 212			
Corn	83	90	2.0
Soybeans	82	72	17.0
Trees	54	68	12.0

In general, there was considerable confusion between trees and soybeans in Segments 203 and 212. Almost half the soybean area in Segment 203 was classified as trees and over 20% of the tree areas in Segment 212 were classified as soybeans. This is borne out by the false alarm rates listed in Table 6.

It is also noreworthy that for Segments 203 and 212 there were no gross changes in results for edge areas of the data. However, in Segment 204, classification accuracies for soybeans and trees fall off sharply for the edge areas. The reasons for this will be explored a little further in this section.

In investigating the above results, several other phenomena were also noticed. For one, many of the ratio channels were found to contain no useful discrimination information; i.e., all object classes of interest generated the same ratio signal.

It appears that this is caused, in part, by the fact that many object classes have the same spectral shape (although different magnitudes of signals). In calculating the ratios, the information regarding relative magnitudes of signals is knowingly discarded. Recognition is accomplished using only information regarding relative spectral characteristics between adjacent channels. If the spectral shapes of different object classes are similar, then the ratio transform results in channels that contain no information for discrimination. Another facet of this problem might be that, in some instances, spectral shapes are dissimilar, but the presence of an additive (path radiance) term serves to overshadow and obscure any small differences in shape.

Secondly, it was noticed that most of the discrimination was being done on the basis of one ratio channel, namely the ratio of data from two spectral bands: .72-.92 μm and .69-.72 μm.

Thirdly, it was observed that this ratio channel exhibited a marked angular variation at extreme scan angles. Figure 7 shows this graphically, again using the mean signals for three object classes at many scan angles to display it. The reason for the poor recognition at the edges of Segment 204 is apparent, but the cause is not.

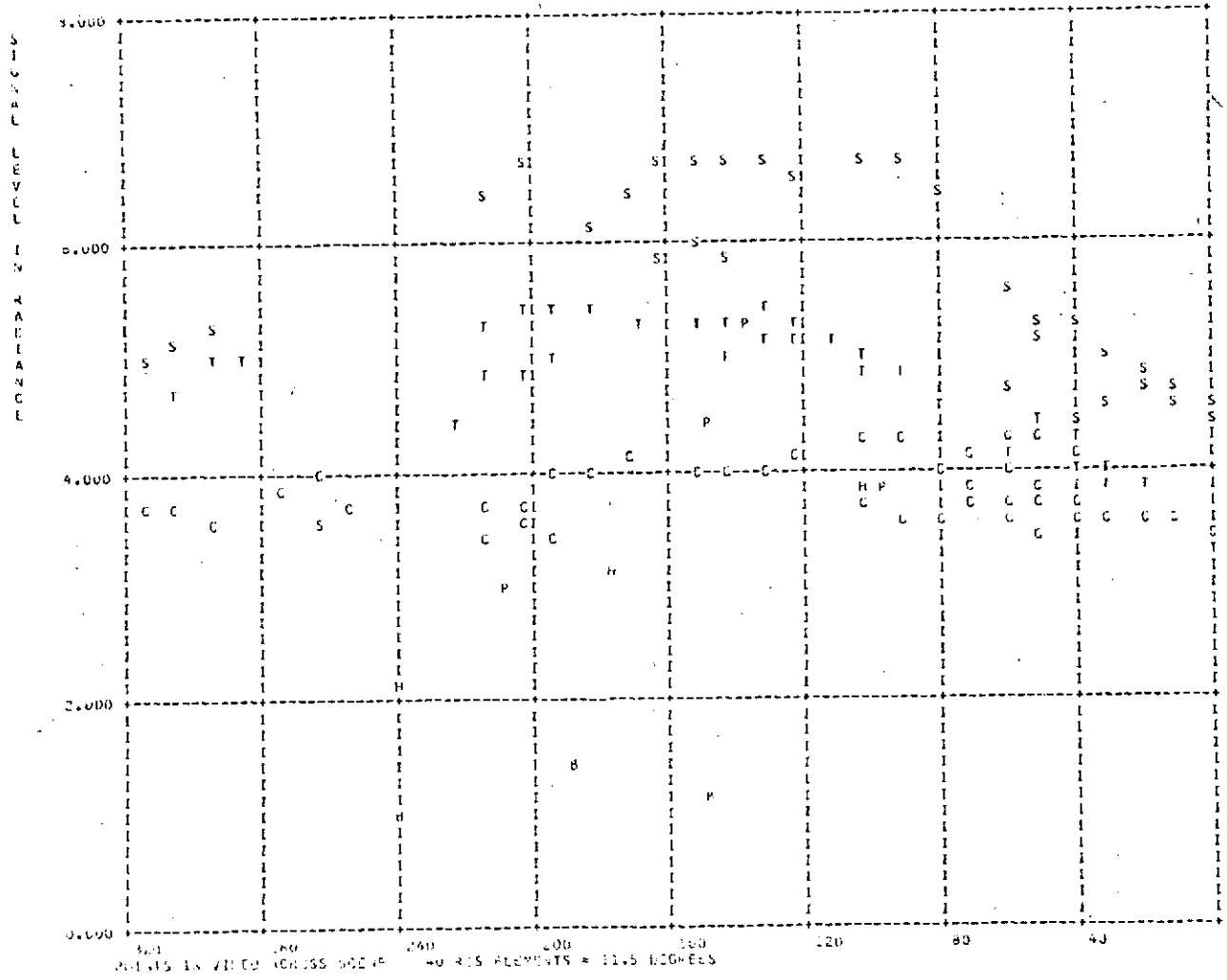

FIGURE 7. VARIATION OF SPECTRAL RADIANCE AS A FUNCTION OF SCAN ANGLE FOR CORN, SOYBEANS, AND TREES FOR SEGMENT 204, MISSION 43M.
Ratio of adjacent channels transform.
Channel is ratio of (0.72-0.92 μm)/(0.69-0.72 μm) wavebands.

We had, previously in this section, glossed over the effects of the additive term in calculating the ratios for adjacent channels. Let us go back and examine it again. For any given angle, let

$$L_{p_i} = q_i \rho_{i,j} E_i T_i g_{i,j}$$

where q_i is some scale constant. Thus, Equation 4.2 can be rewritten as

$$R_i = \frac{\rho_{i+1,j} E_{i+1} T_{i+1} g_{i+1,j} [1 + q_{i+1}]}{\rho_{i,j} E_i T_i g_{i,j} [1 + q_i]} \tag{4.5}$$

$$\approx \left[\frac{\rho_{i+1,j}}{\rho_{i,j}}\right] * [\text{CONSTANT}] * \left[\frac{1 + q_{i+1}}{1 + q_i}\right] \tag{4.6}$$

It is evident that if the right hand term is not constant for all scan angles, a certain angular variation will still exist. We carried out calculations using the ERIM radiative transfer model to determine the form of the variations to be expected for the Segment 204 data set. For the pair of channels, .69-.72 μm and .72-.92 μm (corresponding to spectrometer channels 7 & 8, respectively), it was found that the ratio

$$\left(\frac{1 + q_8}{1 + q_7}\right)$$

decreases with increasing scan angle. A plot of this is shown in Figure 8; the similarity between this and Figure 7 is apparent.

In accordance with the above investigation, it was felt that recognition accuracy using the ratio transformation could be increased, if the effects of path radiance could first be reduced or eliminated. Accordingly, several methods to eliminate the path radiance term were investigated.

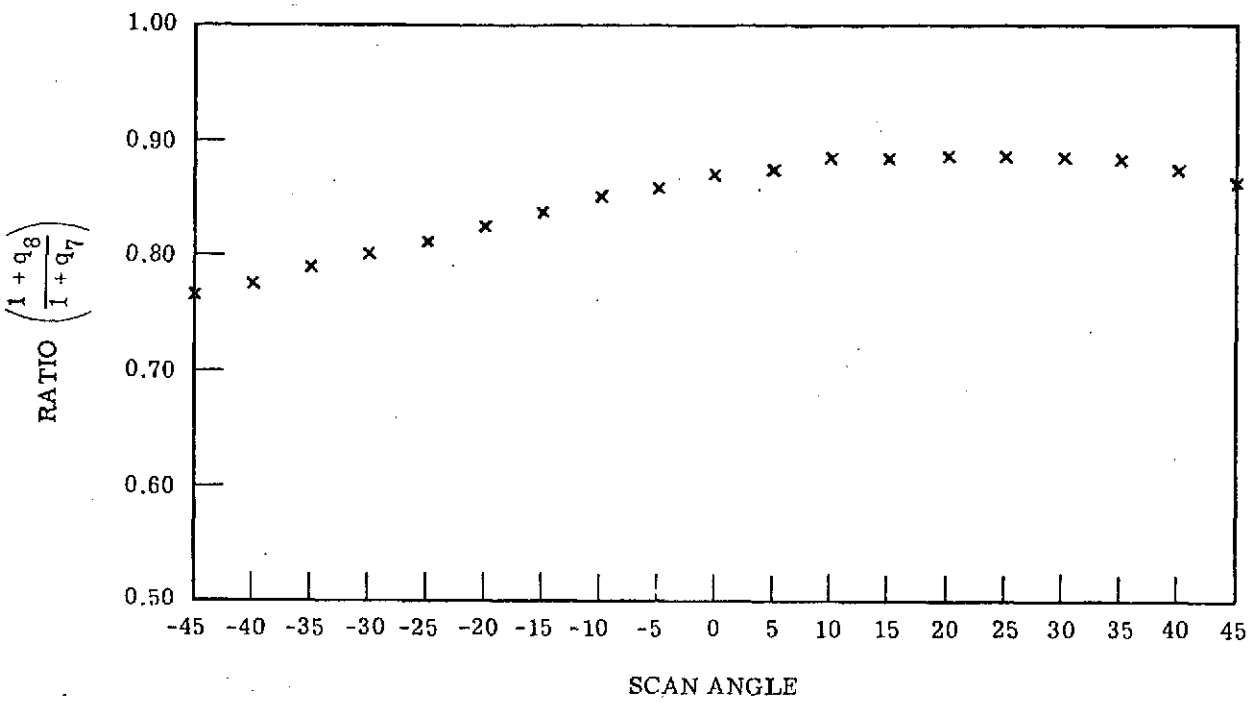

FIGURE 8. PLOT SHOWING EFFECT OF PATH RADIANCE ON CALCULATION OF RATIO OF ADJACENT CHANNEL TRANSFORM FOR RATIO CHANNEL $\left(\frac{0.72\text{-}0.92\ \mu m}{0.69\text{-}0.72\ \mu m}\right)$

4.1.1.1 ESTIMATION OF PATH RADIANCE USING THE ERIM RADIATIVE TRANSFER MODEL

We first attempted to eliminate the path radiance contributions by subtracting the model calculated path radiance from the data. If the angular variation were due entirely to atmospheric effects it was expected that the resulting mean plots of $(L_o - L_p)$ would be inverted parabolas, since the dominant angle dependent term would be T (transmittance). It turned out, however, that even after subtracting the calculated path radiance the shape of the plots were still positively parabolic. This is shown in Figure 9 for the 0.56 μm - 0.59 μm wave-band.

The effect of decreasing atmospheric transmittance at large scan angles would be overshadowed if either the calculated path radiance effects had been under-estimated, or if other multiplicative effects (e.g., bidirectional reflectance) were present. If the latter was the entire reason, the effect of the remaining angular variations would be eliminated if the modified data were classified using the ratio of adjacent channels transformation. The data were transformed in this manner. Mean plots of these transformed signals revealed that the ratio data exhibited the same characteristics that were observed in the initial ratio of adjacent channel test. Many of the transformed channels again exhibited small signal ranges such that different object classes could not be differentiated. Also, the mean plot of the ratio of spectral bands $\left(\frac{0.72\text{-}0.92\ \mu m}{0.69\text{-}0.72\ \mu m}\right)$ for this transformation displayed the same angular variation as that seen in the initial ratio transformation of these bands. This can be seen by comparing Figure 10 to Figure 7. The poor results obtained upon classifying the data only reinforced the conclusion that this approach did not adequately reduce the angular variations in the data.

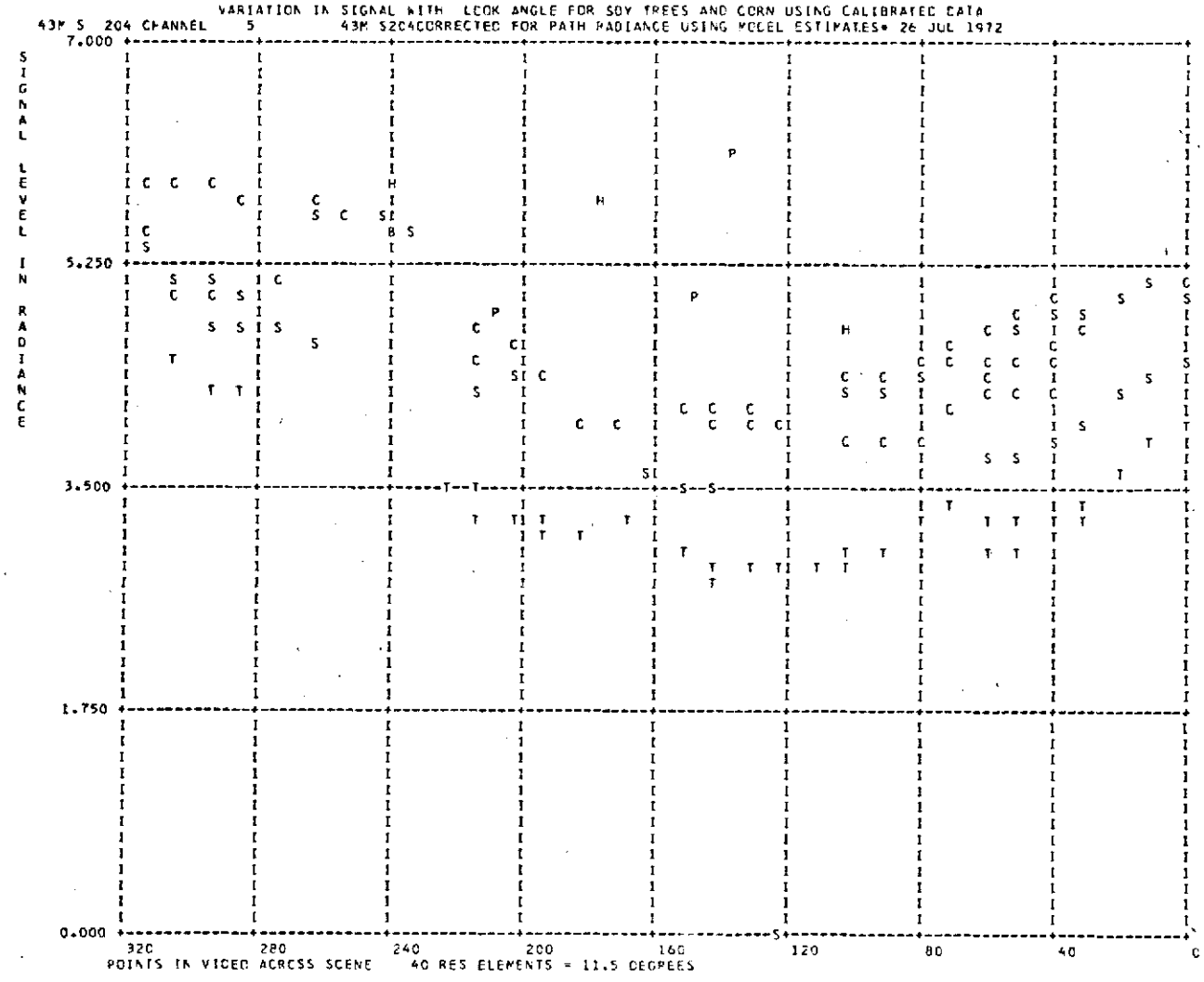

FIGURE 9. VARIATION OF SPECTRAL RADIANCE AS A FUNCTION OF SCAN ANGLE FOR CORN, SOYBEANS, AND TREES FOR SEGMENT 204, MISSION 43M. Data transformed by subtraction of path radiance as calculated by the ERIM radiative transfer model. Channel = 0.56-0.59 μm.

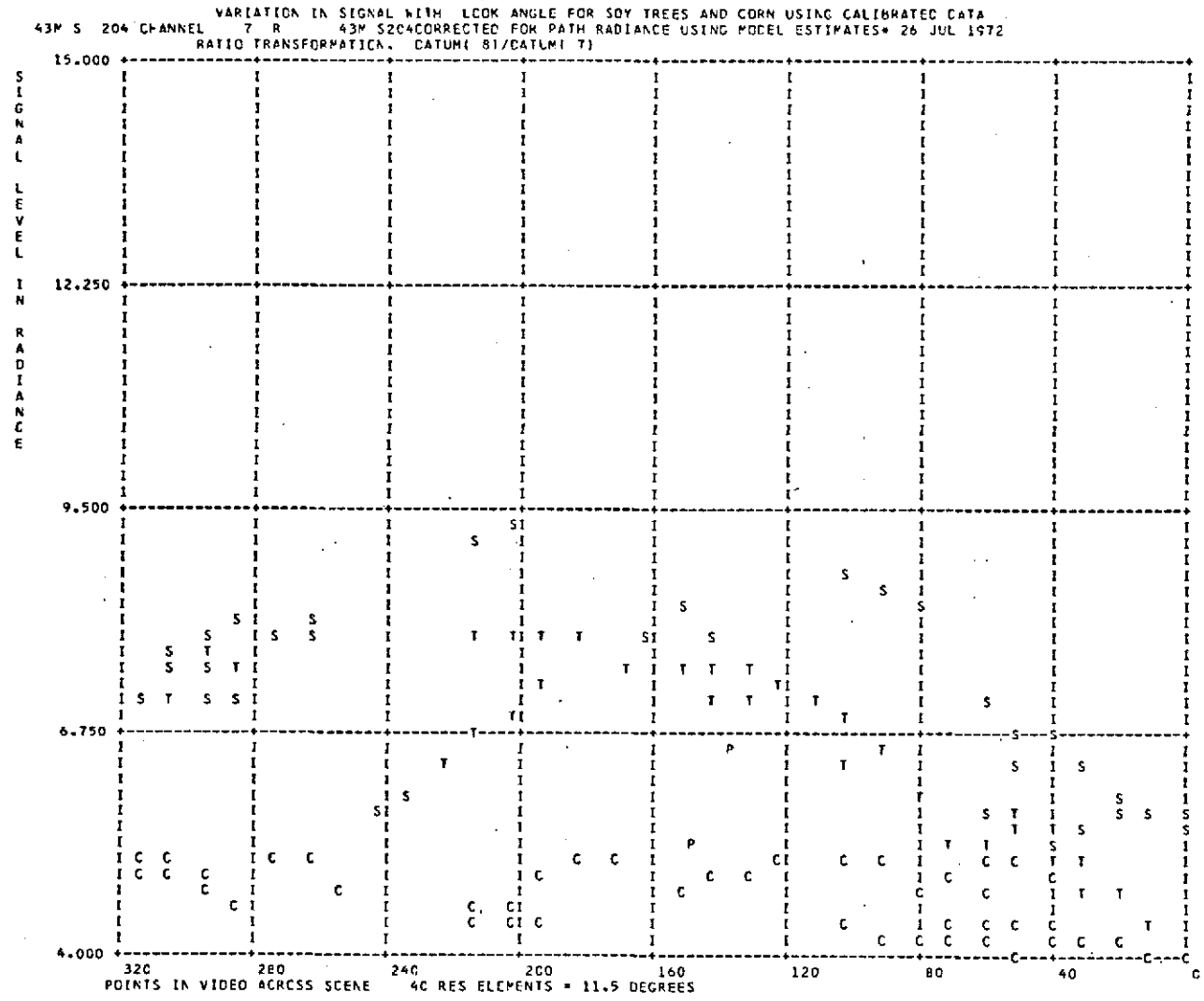

FIGURE 10. VARIATION OF SPECTRAL RADIANCE AS A FUNCTION OF SCAN ANGLE FOR CORN, SOYBEANS, AND TREES FOR SEGMENT 204, MISSION 43M. Data transformed by subtraction of path radiance as calculated by the ERIM radiative transfer model and then by ratio of adjacent channels transform.

Channel is the ratio of (0.72-0.92 μm)/(0.69-0.72 μm) wavebands.

The exact reasons for the failure of this approach are not understood at this time. It may have been that the model calculations were not accurate, or that our knowledge of the atmospheric state at the time the data were collected was incorrect. Another cause might be errors in the process by which the data were calibrated. Thus, until the problem can be identified and solved, this method will not be useful.

4.1.1.2. ESTIMATION OF PATH RADIANCE USING THE DARKEST OBJECT METHOD

Another method to estimate the path radiance was tried. Called the Darkest Object Method, it is a means of empirically estimating the additive component at each scan angle in the data. This method is based on the following: If the reflected radiance at any resolution element is close to zero because either the reflectance is close to zero or the incident radiation on the resolution element is small (e.g., the object is in a shadow), then the radiance received at the scanner is essentially all path radiance. Thus, the lowest signal level at each scan angle may be used to estimate the additive correction. This method assumes that there are sources of low reflected radiance at many scan angles in the data. It also assumes that the additive component at each scan angle is constant over the time of data collection.

A measure of the plausibility of the Darkest Object Method is provided in Figure 11. Plotted are the nadir values of the darkest object for Segment 204 and radiative transfer model calculations of path radiance for two atmospheric visibilities: 6 KM and 23 KM. Two things are apparent: One, the spectral shape of the darkest object parameters closely resembles that

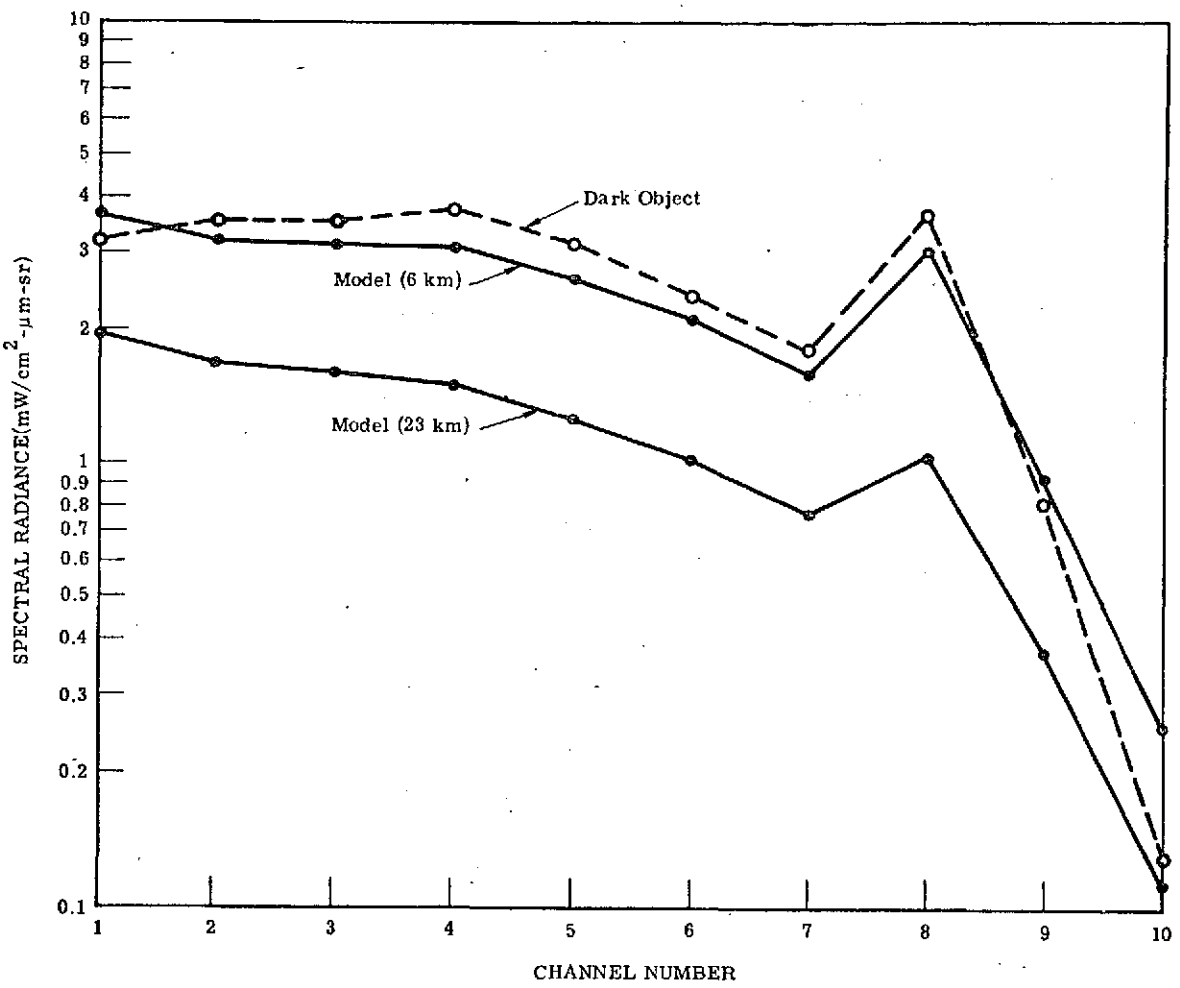

FIGURE 11. SPECTRAL RADIANCE FOR DARK OBJECT AND MODEL CALCULATIONS OF PATH RADIANCE FOR SEGMENT 204 FOR 6 km AND 23 km VISUAL RANGE FOR THE NADIR VIEW ANGLE

of the model path radiance calculation, and secondly, the darkest object approach results in an apparent overestimation of the path radiance, since the visibility at the time of data collection was between 15-20 KM.

As pointed out in the previous subsection, however, there may be errors either in the manner in which the model calculations were carried out or in the calibration processes of the data. Also, it is suspected that ρE may be greater than zero for the resolution elements selected as being darkest which would lead to an overestimation of the additive term. The important point, however, was that the spectral shapes were very similar. Because of this similarity, we felt that it was worth while to continue testing this approach.

The data were processed by subtracting the darkest object values from the data. Plots of these signals means were then generated; an example is shown in Figure 12. Surprisingly, they were not inverted parabolas as had been expected. Instead, in most channels they were fairly level -- very little curve to them at all, and the signals for the three crops were well separated.

The results of classifying the darkest object modified data were very poor, certainly not what had been expected in view of the apparent separability of the object classes. Investigation revealed errors in the training procedure such that the classification results were completely meaningless. It had been our intention to redo this part of the work and to also utilize the ratio of adjacent channels transformation in conjunction with the darkest object approach. However, owing to a shortage of time and funds this was not possible. As a result, the darkest object approach is neither proven nor disproven.

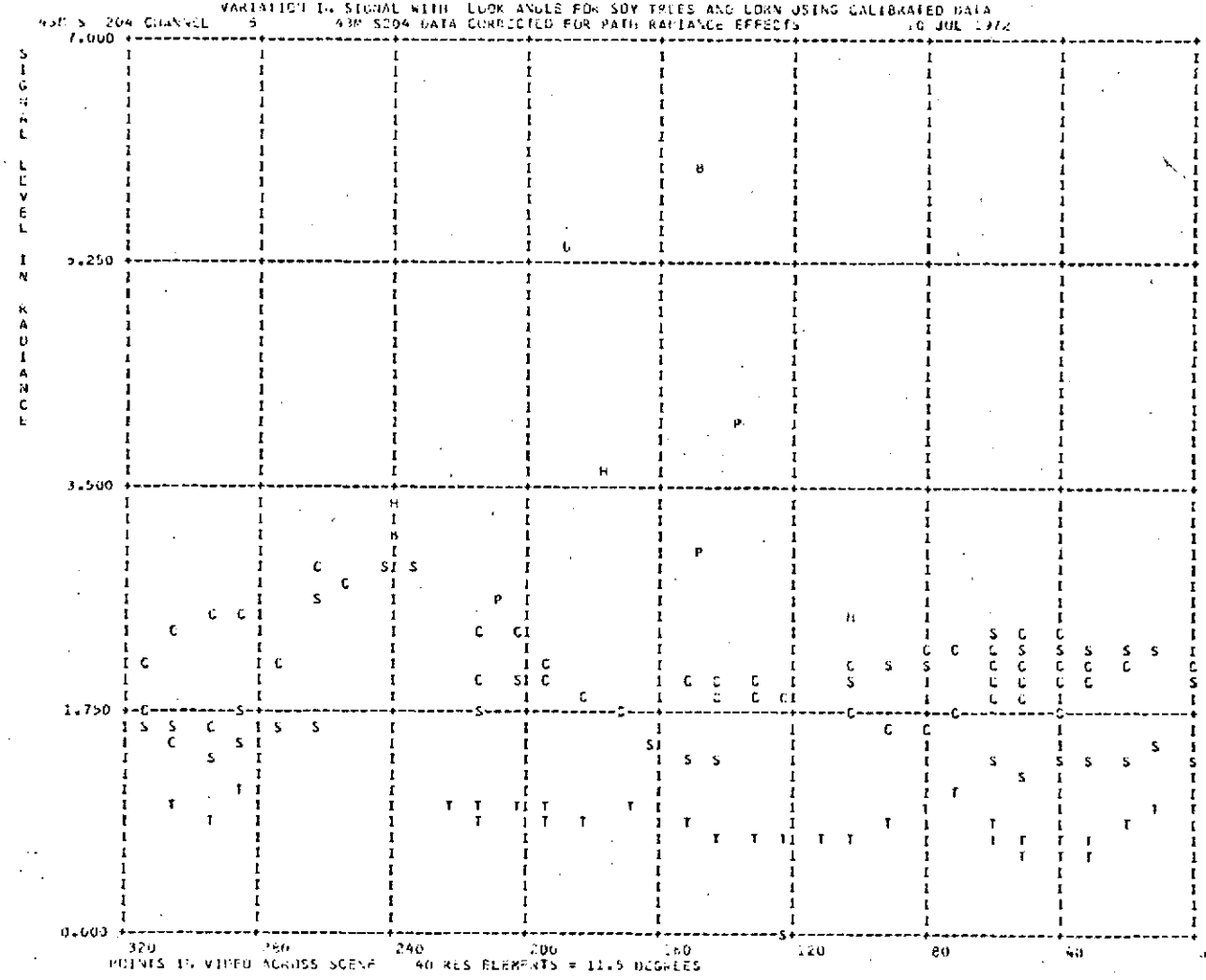

FIGURE 12. VARIATION OF SPECTRAL RADIANCE AS A FUNCTION OF SCAN ANGLE FOR CORN, SOYBEANS, AND TREES FOR SEGMENT 204, MISSION 43M.
Data transformed by subtraction of darkest object values.
Channel = 0.56-0.59 μm.

4.1.2. DIFFERENCE/DIFFERENCE TRANSFORM

One additional method was developed to attempt to account for the path radiance contribution and utilize a ratio transformation. This transformation, called the "Difference/Difference" transform, was developed on the basis of information extracted using the Radiative Transfer Model.

It was observed from plots of path radiance that the spectral shape of the path radiance curve remained relatively constant over a wide range of scan angles and visual ranges for a fixed albedo and sun angle. An example of such a plot is presented in Figure 13, where path radiance for four scan angles for a clear atmosphere is displayed. It will be seen that the assumption of constancy of shape is correct for most channels. However, it does not hold for the relationship between channels 7 and 8. Any channels in the new transformation that use the relationship between channels 7 and 8 would obviously still vary with scan angle, etc, however the other channels of the transformation would be useful.

Thus, assuming that for a given set of solar angles and albedo, the ratio of the path radiance in adjacent spectral bands at all scan angles is approximately constant:

$$\frac{L_{P_i}}{L_{P_{i+1}}} \approx K_{i,i+1} \tag{4.7}$$

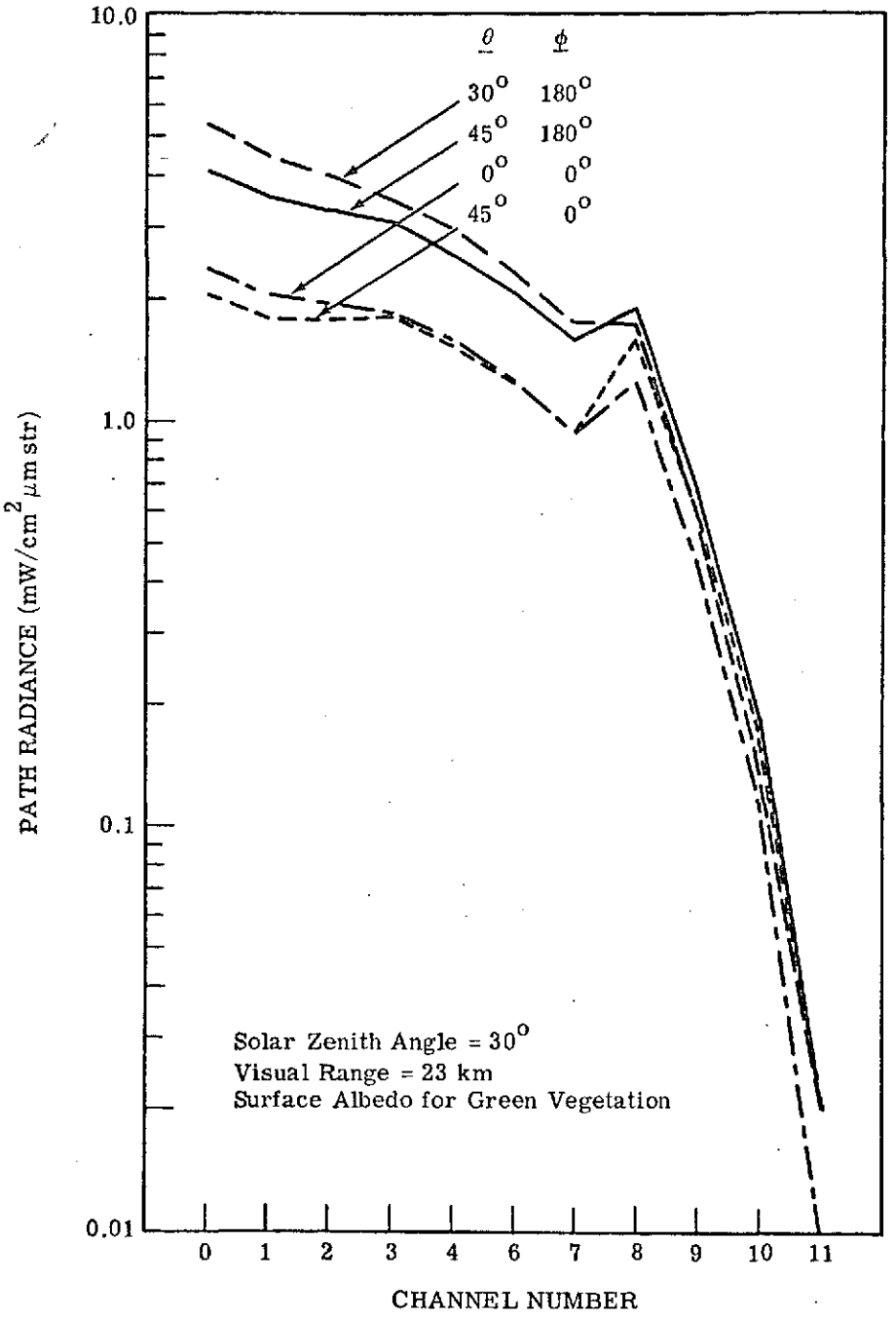

FIGURE 13. SPECTRAL PATH RADIANCE FOR FOUR SCAN ANGLES θ WHERE ϕ IS THE AZIMUTHAL ANGLE BETWEEN THE SUN AND THE PLANE OF SCAN

and assuming for all scan angles that:

$$\frac{\rho_i E_i T_i}{\rho_{i+1} E_{i+1} T_{i+1}} \approx \frac{\rho_i}{\rho_{i+1}} C_{i,i+1} \tag{4.8}$$

as was done for the ratio of adjacent channels transform, a new signature extension transform can be written as:

$$\frac{L_{o_i} - L_{o_{i+1}} K_{i,i+1}}{L_{o_{i+2}} - L_{o_{i+1}} K_{i+2,i+1}} \approx \frac{\frac{\rho_i}{\rho_{i+1}} C_{i,i+1} - K_{i,i+1}}{\frac{\rho_{i+2}}{\rho_{i+1}} C_{i+2,i+1} - K_{i+2,i+1}} \tag{4.9}$$

(where L_o is the radiance sensed at the scanner). The deterministic quantities L_o and K are on the left side of (4.9).

To use the transform the observed radiance for each data point is determined by calibrating the data while the values for K are determined from model calculations using the albedo (e.g., green vegetation in an agricultural scene) which is known to be the predominant background in the scene. The right side of (4.9) includes the albedo-related constants K, the multiplicative constants C and the ratios of adjacent channel reflectances. Therefore, if the assumptions of (4.7) and (4.8) are true, the calculation of the left side of (4.9) for the objects of interest in the scene may provide signatures which are extendable over variations in scan angle, visibility, and perhaps altitude and, accounting for both additive and multiplicative effects.

We tested this transform as we had the ones previously discussed. Results of tests of this transform were very poor. We have already mentioned uncertainties in calibration and model calculations as being possible reasons for poor results.

Another serious problem in this transformation was the large variations in the transformed signals. For many of the object classes, the variation in some of the channels was large enough, in fact, to engulf all the signals in that channel. Problems of this kind are not too surprising when one considers what is the result if the differences in the numerator and denominator are small numbers. The effect of noise in such situations is very serious, causing wild gyrations in the signal levels. For this transform to be useful this problem will have to be overcome.

4.1.3. APPLICATION OF RATIO OF ADJACENT CHANNELS TRANSFORM TO C-3 AREA DATA SET

Before leaving the topic of ratio signature extension techniques, we will report on work that was done on a non-corn blight watch data set.

That the ratio of adjacent channel technique also accounts for along track changes (e.g., changes in irradiance) was demonstrated by the following experiment. From the ERIM archives we selected a data set which contained, in addition to variation with scan angle of the type already encountered, an along track variation. Although it is impossible to state with any certainty the cause of this variation, it is probable that it was caused by changes in atmospheric transmission and/or changes in irradiance at the ground. The data set was collected during a flight over the Purdue University Agronomy farm C-3 area on June 30, 1966 during the late afternoon.

The data set was prepared as usual except that we did not calibrate it in terms of radiance. Recognition processing was carried out using no signature

extension techniques (the untransformed case) and using the ratio of adjacent channel technique. Training for four object classes (corn, soybeans, pasture, wheat) was carried out on the first four fields of this type in the data set. Figures 14 and 15 are recognition maps of the area for the untransformed and the transformed case. Figure 16 is provided as a ground information map.

In the untransformed case, the along track changes were most noticeable in the 7 wheat fields in the data set. The wheat training set was well recognized, but thereafter wheat recognition fell off drastically. Two of the wheat fields were not recognized at all and for two others less than 20% of the data points were correctly classified. All of the wheat fields in the transformed case were well recognized; for five of the fields, better than 90% of the data points are correct and for the other two fields better than 70% of the points were correctly classified. Classification accuracy for corn and soybeans was only about 60% as there was a great deal of confusion between the two crops. In several instances whole fields of corn were classified as soybeans and vice versa.

Such confusion between corn and soybeans is not unexpected early in the growing season. At that time the two crops tend to be spectrally very similar. Also, among young plants, differences in ground cover will result in different spectral characteristics for fields of the same crop. It is probable that for these two training sets, the classification results reflect the percentage ground cover and not the object class present in these fields.

However, the excellent recognition results obtained for the wheat fields indicate that for spectrally distinct object classes the ratio of adjacent channels transformation automatically corrects for along track as well as across track variability.

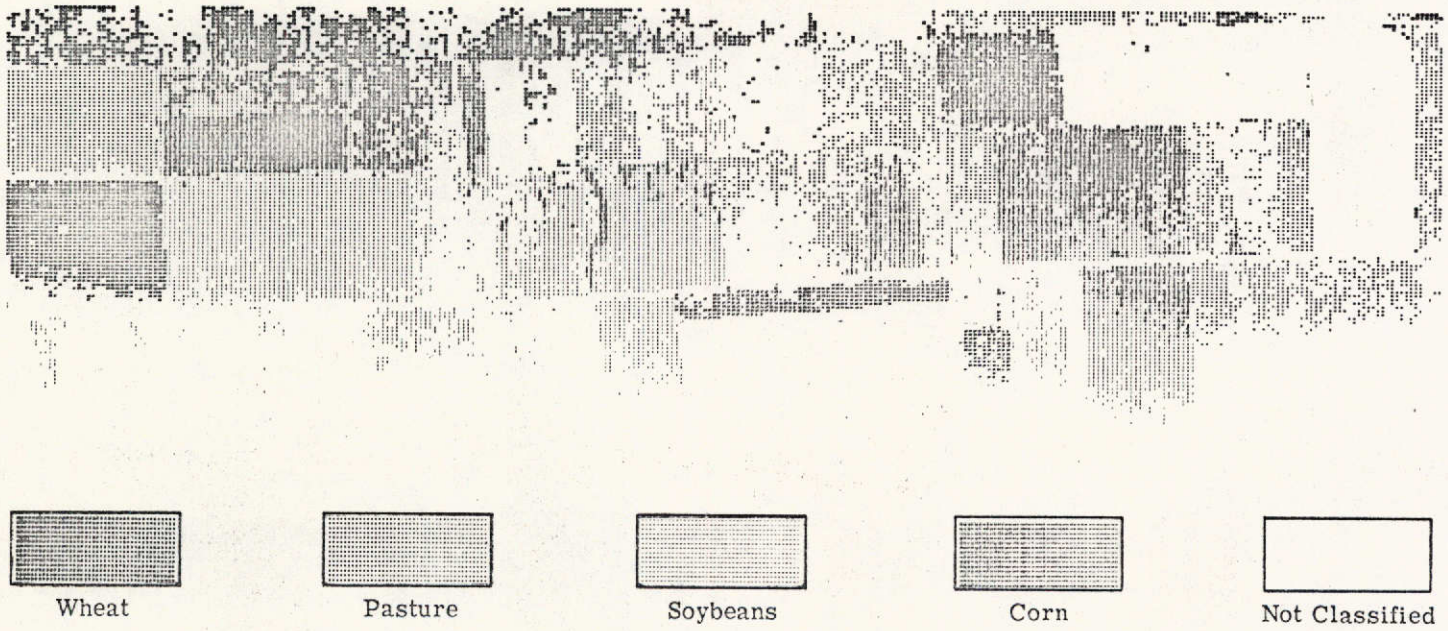

FIGURE 14. RECOGNITION MAP OF C-3 FLIGHT LINE, JUNE 30, 1966. No signature extension techniques were used in processing the data.

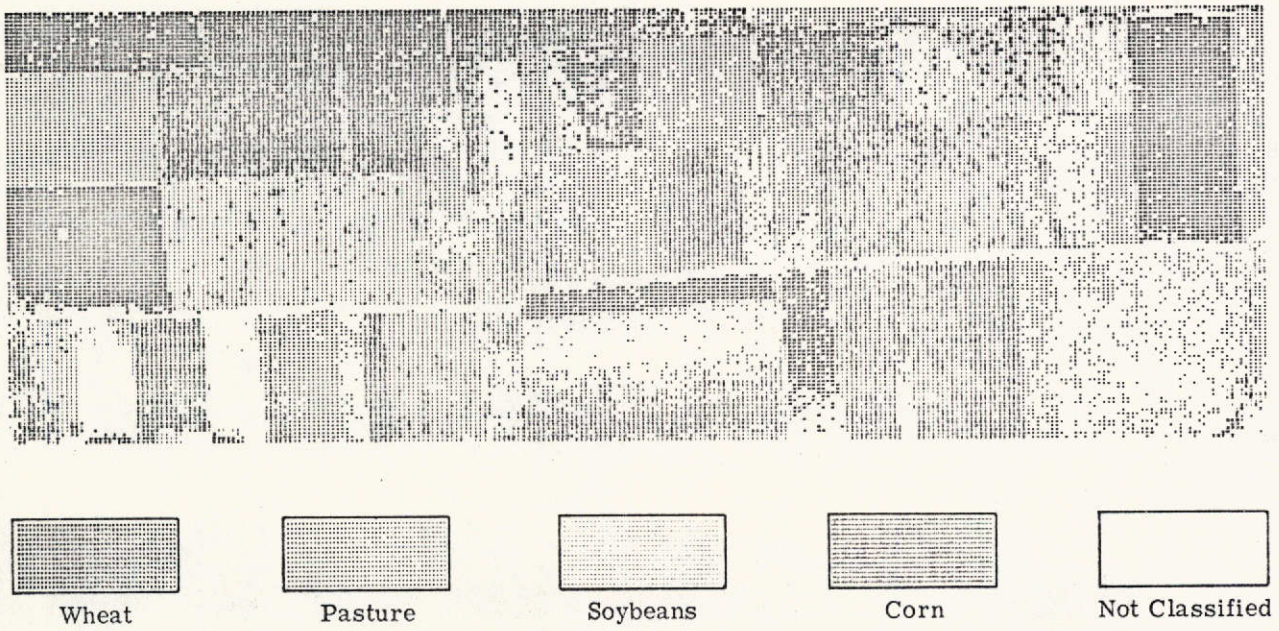

FIGURE 15. RECOGNITION MAP OF C-3 FLIGHT LINE, JUNE 30, 1966. Ratio of adjacent channels signature extension technique used.

LEGEND

W = Wheat
S = Soybeans
C = Corn
A = Alfalfa
P = Pasture
RC = Red Clover
u = Unknown

(Fields Not Labelled are Unknown Crops)

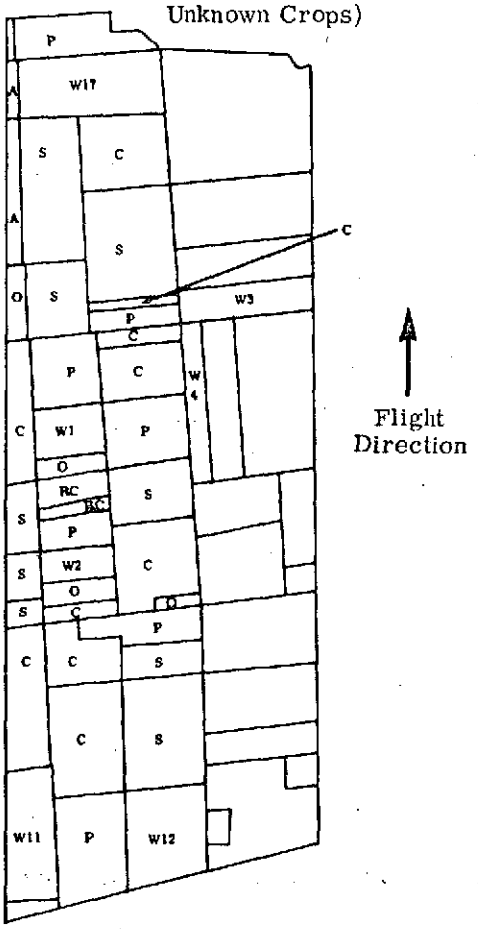

FIGURE 16. GROUND TRUTH MAP FOR C-3 FLIGHT LINE, NEAR LAFAYETTE, INDIANA ON JUNE 30, 1966

4.2. AVERAGE SIGNAL VS ANGLE

This signature extension transformation is different than the ratio transforms already discussed in that here for each scan angle an average correction is computed and then used for the entire data set. The correction function is derived by computing the average signal at each scan angle over the entire data set; to arrive at a smooth correction function, a second order curve is fit to the average signals. This function is indicative of the average angular variation in the data. Obviously, though, for this function to be useful in reducing the angular variations for all objects, the data set being processed must have a quasi-random distribution of all object classes, otherwise the average signals would be scene dependent and would not be an accurate measure of angular variation. One other limitation to this approach is that it will not correct for environmental changes along the flight path. For a data set where changes of this nature occur, the correction values derived by this method will, in general, not yield suitable results (since the correction is an average correction for a widely varying set of conditions). However, the effects of such changes, should they occur, may be substantially reduced during the data preparation phase using the scanner's sky sensor (see Appendix I for a more complete discussion).

The correction function described above may be applied in either of two ways. The correction value at each angle can be subtracted from the data to reduce the additive effects if it is felt that these are the dominant sources of variation; or, the data can be divided by the correction function. This latter approach reduces the effect of multiplicative variants in the data. Prior to correcting the data, the smoothed angular signal is adjusted by utilizing the

signal value at a selected reference angle. When correcting for additive effects, the signal value at the reference angle is subtracted from the smoothed angular signal. As a result, the correction function value at the reference angle is zero. When correcting for multiplicative effects, the smoothed angular signal is normalized by the value at the reference angle.

Separate correction functions were calculated for each of the three segments. An example of the shapes of the correction functions can be seen for two wavebands of Segment 204 in Figures 3 and 4. The three data sets were corrected using the multiplicative mode of correction. Figures 5 and 6 show the effect on the mean crop signals of correcting for angular variation on Segment 204 using this method.

Since the average signal vs angle method does not account for environmental changes between data sets, the signatures from Segment 204 could not be applied directly to the other two data sets. However, it is possible to easily develop scaling factors such that the signatures from one data set can be scaled to the signal levels of a second data set. For both data sets, the average signal at the reference scan angle is known. The ratio of these average signals provides the necessary scaling factors. This method requires that both data sets have about the same distribution of object classes.

The approach described above was employed to identify the scale factor adjustments necessary for the application of Segment 204 signatures to Segment 203 and 212 data. All these data sets were then classified. Excellent recognition results were obtained for all three data sets. Per cent correction classification for test fields in Segments 204 and 212 exceeded 90%, while for Segment 203, it was near 85%. Except for high tree false alarm rates for Segments 203 and 212,

the false alarm rate is very low. A complete listing of recognition results and false alarm rates is provided in Table 7.

TABLE 7. CLASSIFICATION RESULTS FOR AVERAGE SIGNAL VERSUS ANGLE TRANSFORMATION

All Data Classified Using Signatures From Segment 204

	% Recognition for Test Fields		% False Alarm Rate for Test Fields
	Middle	Edge	
Segment 204			
Corn	97	98	1.5
Soybeans	98	88	2.6
Trees	100	88	0.8
Segment 203			
Corn	93	81	1.1
Soybeans	70	86	3.1
Trees	94	97	37.0
Segment 212			
Corn	89	87	0.75
Soybeans	89	91	1.6
Trees	98	99	20.4

4.3. U-V TRANSFORMATION

This transformation was first suggested and developed by R. Crane of ERIM.[9] It empirically computes both additive and multiplicative corrections for each data set. In this technique, pairs of fields or regions exhibiting different spectral reflectances are utilized to calculate scan angle dependent

multiplicative (U) and additive (V) correction functions, normalized to some reference angle. The data is then corrected to match the conditions at that reference angle. Just as in the previous transform, the same correction functions are used for each scan line of data and the extension of signatures to other areas is accomplished by scaling the signatures according to parameters defined by the correction function.

Because of time limitations, it was possible to process and analyze only Segment 204 using this approach. The correction functions were based on areas representing three object classes (three pairs of different reflectances). The method combines many fields of the same class to cover a wide range of scan angles. Accordingly, the fields used to compute the corrections for Segment 204 were the training fields for corn, soybeans and trees supplemented by fields of each of these object classes at scan angles greater than $+30^{\circ}$ and less than -30° from nadir.

TABLE 8. CLASSIFICATION RESULTS FOR U-V TRANSFORMATION FOR SEGMENT 204

% Recognition for Test Fields	Corn	Soybeans	Trees
Middle	95	89	96
Edge	92	70	55
False Alarm Rate for Test Fields	4.4	3.9	3.7

The results of recognition processing given in the table above are fairly good although it is apparent that recognition accuracy has decreased at large scan angles. The corrections calculated by this method increase or decrease very

rapidly for large off nadir scan angles. As a result, the accuracy of extrapolations is questionable outside of the angular scope of the areas used for the calculations. This is in agreement with other investigators' findings.

The conclusions to be drawn regarding the "U-V" transform are that it does not perform equitably over all scan angles. Also it requires some amount of ground information for each data set processed. One of the real advantages of the U-V method is that it computes corrections for both additive and multiplicative effects.

4.4. COMPARISON OF SIGNATURE EXTENSION TECHNIQUES

In Figures 17, 18, and 19, the results for the various signature extension techniques are compared for Segments 204, 203, and 212, respectively. As can be seen in examining those figures, the best results are obtained for the average signal versus angle transform. The results for the ratio of adjacent channel transform were not quite as good. The results of experiments to estimate the path radiance and thus correct the data for both additive and multiplicative effects were unsuccessful. However, this may have been due to subsidiary influences and not a true indication of the value of these approaches.

The untransformed results for Segment 204 show how variation in the data as a function of scan angle can affect classification performance. Most of the data viewed with scan angle greater than 30° was not correctly classified for this test case. However, use of preprocessing transforms for Segment 204 produced results for edge areas at the same level of accuracy as that obtained in the middle areas. As previously noted, there is some fall-off of recognition at the edges of Segment 204 for the ratio of adjacent channels transform. The average signal vs angle transform

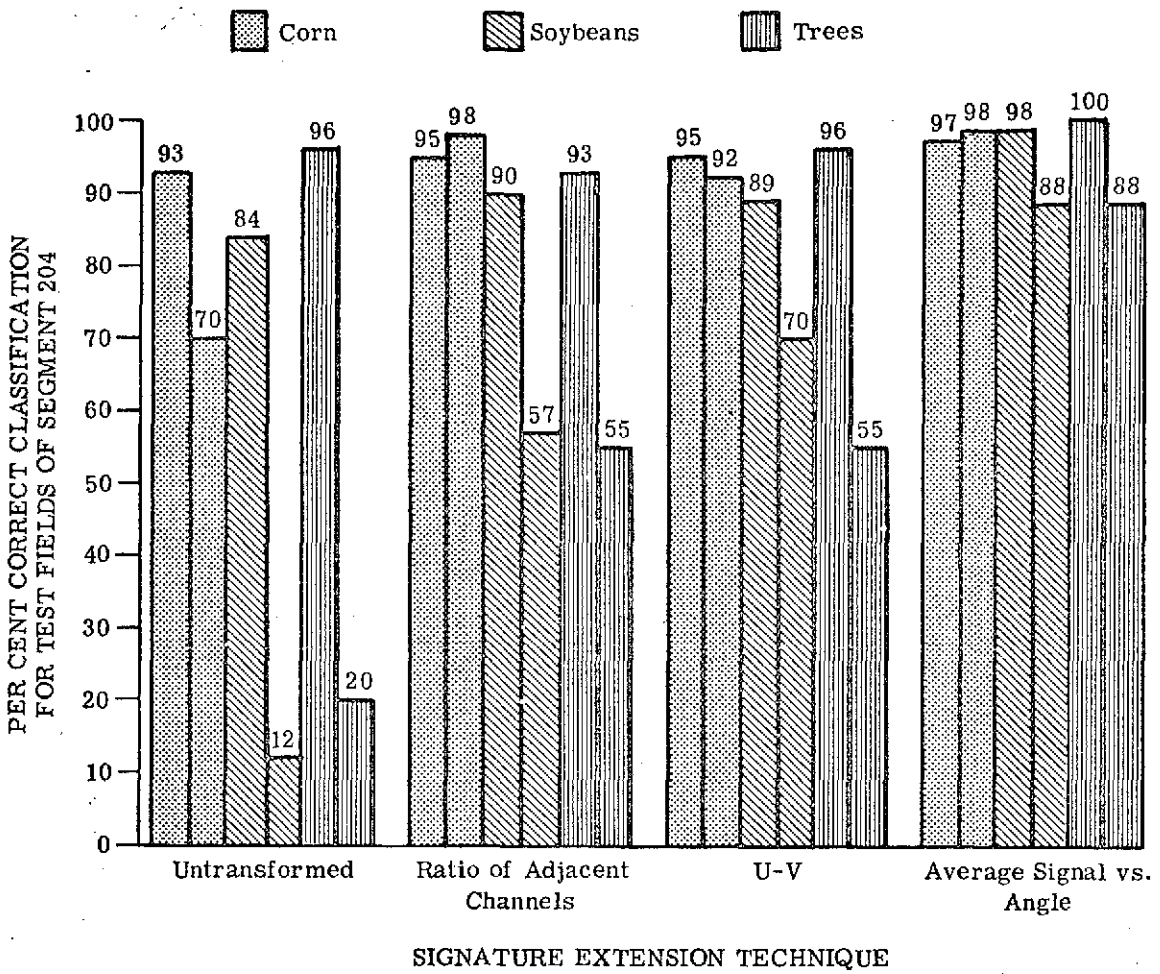

FIGURE 17. COMPARISON OF CLASSIFICATION ACCURACY FOR FOUR SIGNATURE EXTENSION TECHNIQUES FOR SEGMENT 204, MISSION 43M, 1971. For each category, left bar refers to middle fields and right bar refers to edge fields.

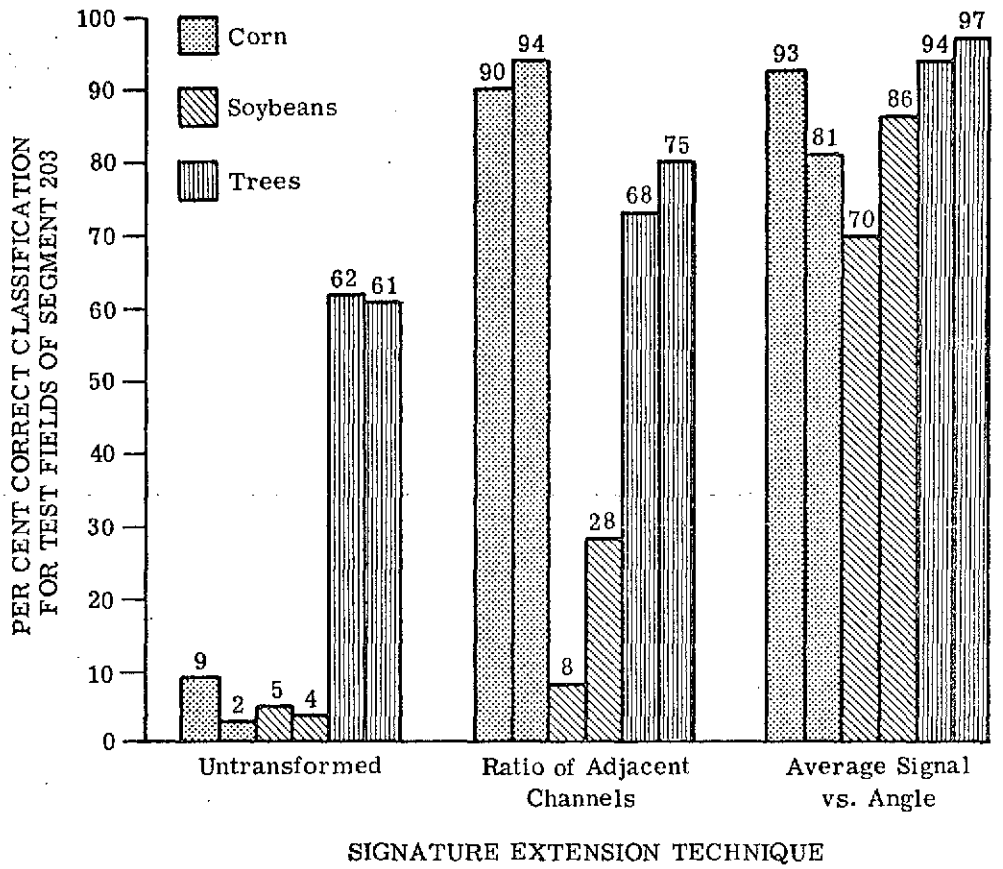

FIGURE 18. COMPARISON OF CLASSIFICATION ACCURACY FOR THREE SIGNATURE EXTENSION TECHNIQUES FOR SEGMENT 203, MISSION 43M, 1971. For each category, left bar refers to middle fields and right bar refers to edge fields.

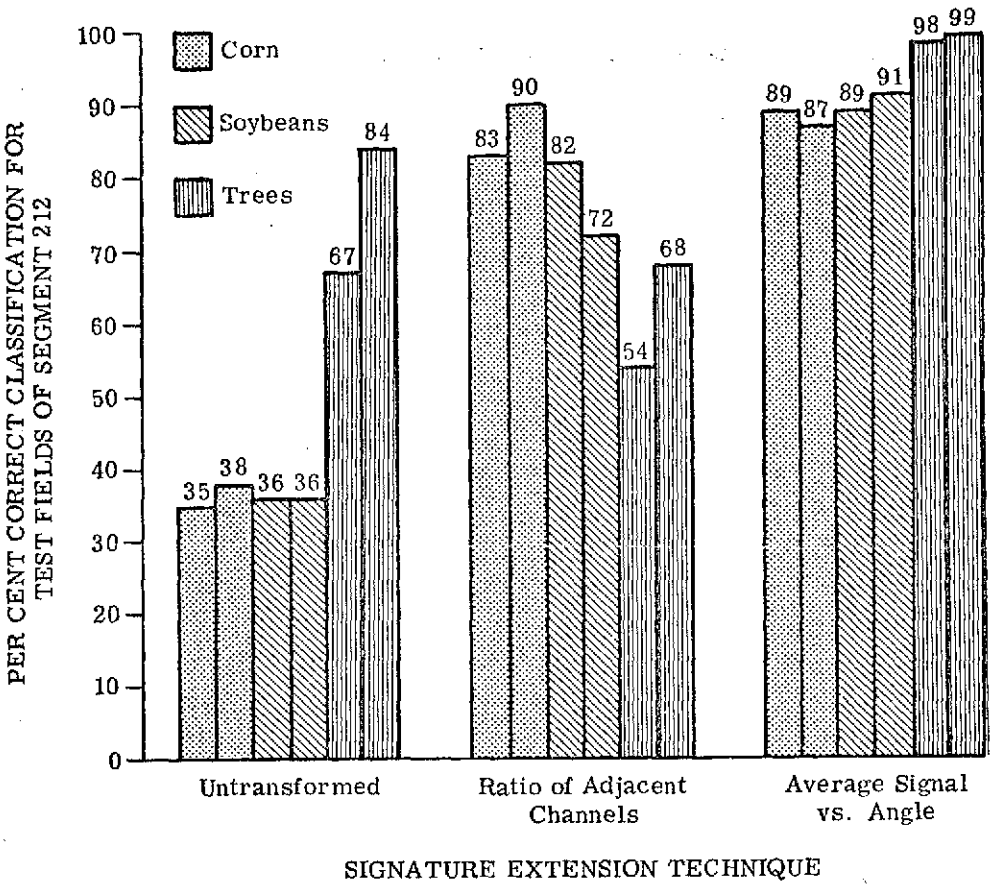

FIGURE 19. COMPARISON OF CLASSIFICATION ACCURACY FOR THREE SIGNATURE EXTENSION TECHNIQUES FOR SEGMENT 212, MISSION 43M, 1971. For each category, left bar refers to middle fields and right bar refers to edge fields.

yields results that do not fall off as much in the edge areas. For Segments 212 and 203 there was not much distinction between middle and edge results.

In reviewing the false alarm rates quoted earlier in this section, it was noted that there was a very high false alarm rate associated with the tree category for both Segments 203 and 212. Aside from the trees, the false alarm rates for all the transformations were low, especially for the average signal versus angle transformation.

In summary, the point to be made here is that the accuracy of classification increases substantially with the use of signature extension techniques. One small group of signatures extracted from an isolated area can be used to successfully process many data sets, despite the fact that these data sets may be 50-100 miles distant and collected several days apart.

5

CONCLUSIONS AND RECOMMENDATIONS

We have shown that for multispectral scanner survey systems to be effective in an operational environment, approaches other than those which have been employed during the feasibility demonstration stage will be required. We have discussed two suggested approaches: the use of clustering and the development and use of signature extension techniques. Based on evidence we presented, it is our feeling that the clustering approach alone will not provide for both cost reductions and accuracy in an operational situation. The use of signature extension techniques, perhaps, but not necessarily, in concert with clustering, seems to show a great deal of promise for satisfying the requirements of an operational multispectral scanner resource survey system.

Several of the signature extension techniques tested yielded good to excellent results. At the present time, we do not have a universally applicable and optimum signature extension technique. We have found that not all the techniques yield good results on all data sets; we have a need to establish criteria for determining when a given technique is useful and when it isn't. Further research on this topic should address itself to these points. We hope eventually to establish a universally applicable signature extension technique.

APPENDIX I
ERIM DIGITAL MULTISPECTRAL DATA PROCESSING SYSTEM

This appendix presents the ERIM data processing system as employed during this study. Figure A-1 shows the general flow chart of the data processing.

The initial process is to convert the data from the analog format it is originally recorded in to a digital format. Preparatory to the digitization, the analog tape is previewed for excessive noise, corrected for misregistration of channels on the tape (due to tape recorder head misalignment problems, etc) and A/D parameters are determined.

All 12 channels recorded by the M-7 scanner were digitized. (These are listed in Table A-1 with the corresponding wavebands.) Each scan line of data was digitized. However, the entire scan line was not digitized--only the specified area of the scene and certain calibration information. The calibration information measured for each scan line is:

"dark level"	-	viewing the dark interior of the scanning housing
"sky sensor"	-	incident radiation on a diffuse opal glass on the top of the aircraft
calibration lamp	-	radiance-transfer standard
cold plate	-	source of cool, known temperature
hot plate	-	source of hotter, known temperature

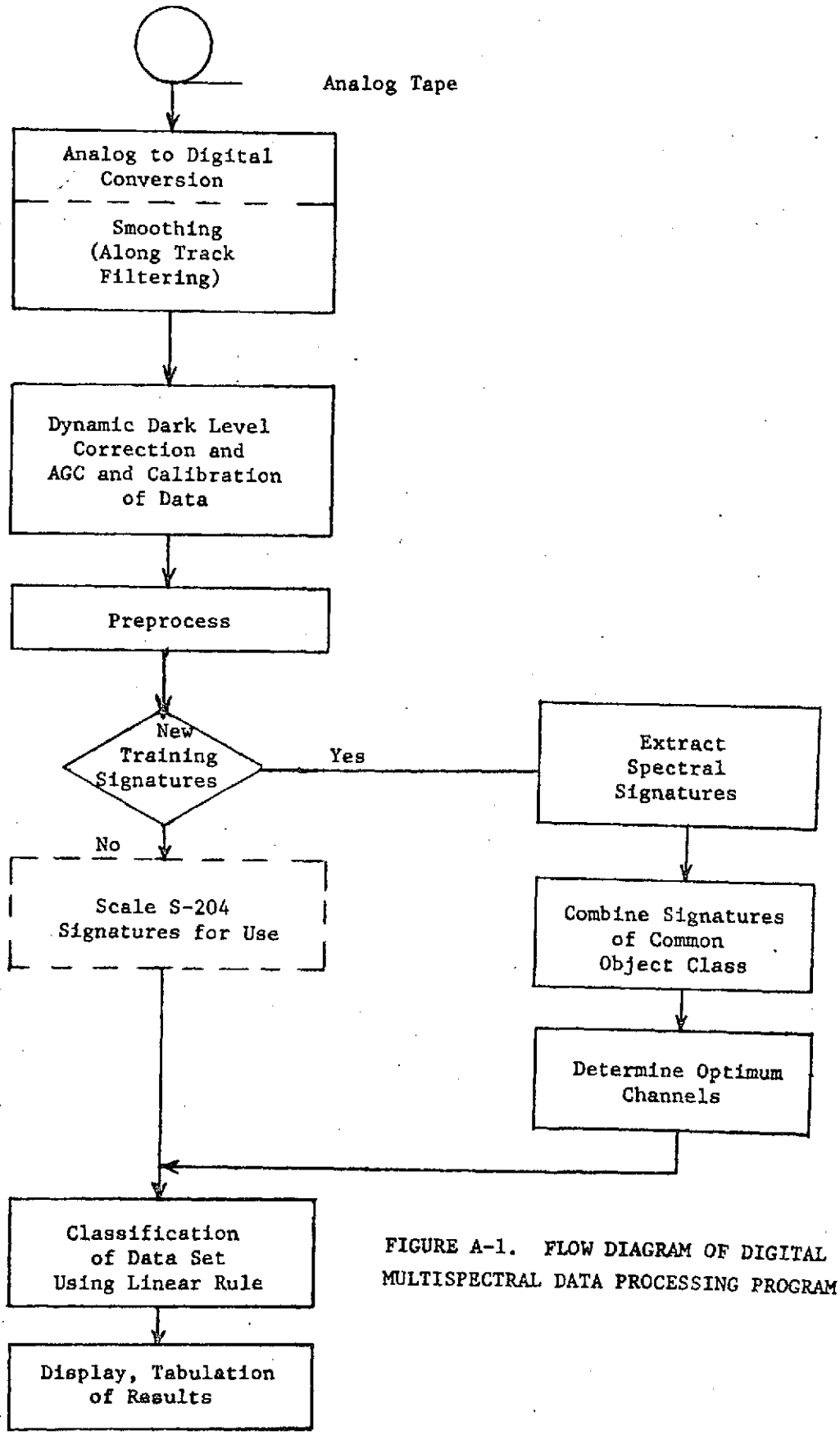

FIGURE A-1. FLOW DIAGRAM OF DIGITAL MULTISPECTRAL DATA PROCESSING PROGRAM

TABLE A-1. TABLE OF M-7 SCANNER WAVEBANDS

Detector	Data Channel	Waveband
SPECTROMETER	1	.469 - .486
	2	.486 - .506
	3	.508 - .531
	4	.534 - .560
	5	.560 - .592
	6	.592 - .626
	7	.630 - .672
	8	.694 - .896
3-Element Near IR Detector	9	1.08 - 1.30
	10	1.50 - 1.85
	11	2.10 - 2.58
Thermal	12	9.3 - 11.7

TABLE A-2. TABLE OF TRAINING SETS

Object Class	Number of Fields	Total Number of Data Points	Largest	Smallest
Corn	7	6691	1672	390
Soybeans	4	3078	1320	288
Pasture	4	2127	816	300
Cut Hay	3	1362	816	150
Bare Soil	3	2207	1425	286
Trees	4	2836	930	352
Growing Hay	4	2113	1150	180

Before proceeding, several facets of the M-7 scanner should be understood.[1] Data gathered at an altitude of 5,000 feet results in approximately a 5 fold redundancy--that is, each infinitesimal area on the ground is scanned in 5 successive scan lines. Also, the three different detector units of the scanner - spectrometer, 3 element near IR and thermal have different resolving capabilities in the along track (flight) direction. The spectrometer has 2 milliradian (MR) resolution; the three element IR detector has 4 MR resolution and the thermal detector has 3.3 MR resolution. One other eccentricity of the scanner is that the three elements of the near IR detector do not have a common line of sight. The three elements are arranged in a linear array. Thus, as the scan mirror rotates, the projection of the array on the ground rotates also. The result is that at large scan angles the three detectors do not image the same ground area. A solution to this problem of bringing all the bands into better registration is to use a data averaging technique.

So it is that the next step in the data processing flow is a smoothing (or filtering) operation. This is the averaging of the data at each scan angle over several successive scan lines. The effect of this along track averaging is to coarsen the effective resolution so that each channel of data then views more of the same ground area. Similarly increasing the size of the ground patch being viewed brings the three elements of the near IR detector into closer registration. Also, the use of averaging techniques significantly increases the signal to noise ratio in the data.

---

[1] For a more complete discussion of this topic, see "Detailed Interpretation and Analysis of Selected Corn Blight Watch Data Sets", by R. F. Nalepka, J. P. Morgenstern and W. L. Brown, Fourth Annual Earth Resources Program Review, NASA/MSC, Houston, Texas, January 1972.

Thus, the redundancy in the data is utilized to reduce these different instrumental effects in the data. For the data sets reported here, every group of 8 lines were averaged together. The effective size of resolution elements at nadir (for data collected at an altitude of 5000 feet) was about 25 feet square. Currently, the A/D conversion and the smoothing are performed during the same operation.

Smoothing, however, does not take care of all the instrumental effects in the data. Effects due to lack of stability in the offset and gain of the data collection system are still inherent in the data.

The next processing step is designed to eliminate the last of these instrumental effects. As previously mentioned, the A/D conversion process includes the signals generated when several calibration sources are viewed. Signals generated for each scan line from the "dark level" are indicative of the offset applicable to that scan line. Similarly, monitoring of signals representing the calibration lamp will indicate changes in system gain. Additionally, the signals from the sky sensor may be monitored to indicate either changes in system gain or changes in illumination at the flight altitude. (For this latter, one must be careful that any changes are not associated with the aircraft rolling.)

Thus, the data in all but the thermal channel were clamped to the dark level and scaled (normalized) to the calibration lamp. The thermal channel was treated by clamping to the hot plate. All clamping and scaling values were calculated for each data line from calibration signals for that line. The calibration of the data was done concurrently with the scaling operation.

At this point in the data processing, the preprocessing approach being tested was applied; then the training signatures were readied. If the data set were Segment 204, this involved extracting signatures and combining them. If the data set being processed was either Segment 203 or Segment 212, then the appropriate signatures were, if necessary, processed (scaled) for use on these data sets. This procedure has already been treated in the text.

For Segment 204, the training procedure was as follows. First, a one mile square area of Segment 204 had been chosen for extracting signatures. The particular area chosen was selected because of the number and variety of object classes contained therein. Table A-2 on Page 60 shows the number of fields of each object class for which signatures were extracted.

For each of the seven object classes, the group of signatures for that class was statistically combined to yield one signature that encapsulated the original signatures for that object class. This is done to account for field to field variations occurring within any object class. By sampling several fields and then combining them, the resulting signature is more representative of the whole object class and not just of one sample of that object class. In combining them, all signatures are given equal weight; they are not weighted proportionally to the number of data points they represent.

Optimum channels for the set of combined signatures were then selected. The channels were chosen by a digital computer program which uses an algorithm based on calculations of pairwise probability of misclassification, based on the use of a linear decision rule.

The next step was the classification of the data set. The seven signatures described above were used to train the computer and the best six channels as chosen were used by the decision rule. The decision rule employed was the linear rule developed by Crane and Richardson.[9] The linear rule is used because it is faster than the more usual quadratic classifier (for this case it was three to four times faster). Or to put it another way, use of the quadratic classifier would have necessitated a reduction in the number of channels used for classification in order to process the data in the same amount of time. The ability to use more channels of information for the time used definitely increased the classification performance.

The classification process utilized also differed from normal pattern recognition techniques in one other regard. This is in the manner in which data points are determined to be alien to any of the training sets. Such points are called "not classified" or unrecognized points. This is determined as follows:

For each data point, one of the training distributions is selected as being most likely that the data point would have come from it. The probability density function for this data point-training set pair is then calculated. This number may then be translated--using a table of the χ^2 -- into the probability that the point came from the training distribution in question. Normally, a minimum allowable probability (e.g., 0.001) is specified and the classification program rules each data point as classified or unclassified depending on whether the calculated probability is greater than or less than the prescribed minimum.

In the current processing scheme, however, it is not handled in this manner. Instead, the output result of the classification process is a two component vector indicating the most likely distribution and the value of the probability density function for each data point.

The distribution of all the pdf values is then studied and the minimum allowable pdf value is selected. This is done by choosing a value such that only 5 or 10 per cent of the data will be declared as "unclassified". This value is then used by the display program in generating a recognition map.

It is necessary to do this because it was found that for many data sets, the minimum pdf value obtained from the χ^2 distribution left as "unclassified" many data points that would have otherwise been correctly classified. This problem was very prevalent in instances where signatures were extended from one data set to another.

The final stage of the processing was an evaluation of the classification results. Recognition maps were generated using minimum pdf values calculated above, and results for the set of test fields in the segment were computed.

The same processing scheme was carried out for each test case run. Exactly the same training areas were used for all cases. For each signature extension method tested, one set of optimal channels were used. In all cases, stringent controls were used to keep the processing of all test cases as similar as possible, so that meaningful conclusions could be drawn from the results of the tests.

REFERENCES

1. Malila, W.A., R.B. Crane, C.A. Omarzu, & R.E. Turner, "Studies of Spectral Discrimination, WRL-IST-U/M Report 31650-22-T, May 1971.

2. Nagy, G., G. Shelton, J. Tolaba "Procedural Questions in Signature Analysis" published in Proceedings of the Seventh International Symposium on Remote Sensing of Environment, Ann Arbor, Michigan, May 1971.

3. Nagy, G. & J. Tolaba, "Nonsupervised Crop Classifications Through Airborne Multispectral Observations", IBM Journal of Research and Development, V. 16, No. 2, March 1972, pp 138-153.

4. Johnston, Dennis A., "Statistical Consideration in an Interactive Graphics Pattern Recognition System", NASA-MSC Internal Note 72-FD-019, Sept, 1972.

5. Su, M.M., "An Unsupervised Classification Technique for Multispectral Remote Sensing Data", Proceedings of the 8th International Symposium on Remote Sensing of Environment, Ann Arbor, Michigan, October 1972.

6. Kriegler, F.J., W.A. Malila, R.F. Nalepka, & W. Richardson, "Preprocessing Transformations and Their Effects on Multispectral Recognition", Proceedings of the 6th International Symposium on Remote Sensing of Environment, Ann Arbor, Michigan, October 1969.

7. Nalepka, R.F., "Investigation of Multispectral Discrimination Techniques", WRL-IST-U/M Report 2264-12-F, January 1970.

8. Crane, R.B., "Preprocessing Techniques to Reduce Atmospheric and Sensor Variability in Multispectral Scanner Data", Proceedings of the 7th International Symposium on Remote Sensing of Environment, Ann Arbor, Michigan, May 1971.

9. Crane, R.B., W. Richardson, R.H. Hieber, & W.A. Malila, "A Study of Techniques for Processing Multispectral Scanner Data", ERIM Report 31650-155-T, January 1973.

10. Nalepka, R.F., J.P. Morgenstern, & W.L. Brown, "Detailed Interpretation And Analysis of Selected Corn Blight Watch Data Sets", Fourth Annual Earth Resources Program Review Meeting, NASA/MSC, Houston, Texas, January 1972.